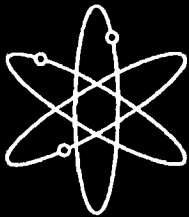
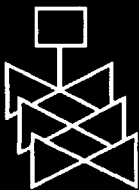




P-CARES: Probabilistic Computer Analysis for Rapid Evaluation of Structures



Brookhaven National Laboratory



**U.S. Nuclear Regulatory Commission
Office of Nuclear Regulatory Research
Washington, DC 20555-0001**



**AVAILABILITY OF REFERENCE MATERIALS
IN NRC PUBLICATIONS**

NRC Reference Material

As of November 1999, you may electronically access NUREG-series publications and other NRC records at NRC's Public Electronic Reading Room at <http://www.nrc.gov/reading-rm.html>. Publicly released records include, to name a few, NUREG-series publications; *Federal Register* notices; applicant, licensee, and vendor documents and correspondence; NRC correspondence and internal memoranda; bulletins and information notices; inspection and investigative reports; licensee event reports; and Commission papers and their attachments.

NRC publications in the NUREG series, NRC regulations, and *Title 10, Energy*, in the Code of *Federal Regulations* may also be purchased from one of these two sources.

1. The Superintendent of Documents
U.S. Government Printing Office
Mail Stop SSOP
Washington, DC 20402-0001
Internet: bookstore.gpo.gov
Telephone: 202-512-1800
Fax: 202-512-2250
2. The National Technical Information Service
Springfield, VA 22161-0002
www.ntis.gov
1-800-553-6847 or, locally, 703-605-6000

A single copy of each NRC draft report for comment is available free, to the extent of supply, upon written request as follows:

Address: U.S. Nuclear Regulatory Commission
Office of Administration
Mail, Distribution and Messenger Team
Washington, DC 20555-0001
E-mail: DISTRIBUTION@nrc.gov
Facsimile: 301-415-2289

Some publications in the NUREG series that are posted at NRC's Web site address <http://www.nrc.gov/reading-rm/doc-collections/nuregs> are updated periodically and may differ from the last printed version. Although references to material found on a Web site bear the date the material was accessed, the material available on the date cited may subsequently be removed from the site.

Non-NRC Reference Material

Documents available from public and special technical libraries include all open literature items, such as books, journal articles, and transactions, *Federal Register* notices, Federal and State legislation, and congressional reports. Such documents as theses, dissertations, foreign reports and translations, and non-NRC conference proceedings may be purchased from their sponsoring organization.

Copies of industry codes and standards used in a substantive manner in the NRC regulatory process are maintained at—

The NRC Technical Library
Two White Flint North
11545 Rockville Pike
Rockville, MD 20852-2738

These standards are available in the library for reference use by the public. Codes and standards are usually copyrighted and may be purchased from the originating organization or, if they are American National Standards, from—

American National Standards Institute
11 West 42nd Street
New York, NY 10036-8002
www.ansi.org
212-642-4900

Legally binding regulatory requirements are stated only in laws; NRC regulations; licenses, including technical specifications; or orders, not in NUREG-series publications. The views expressed in contractor-prepared publications in this series are not necessarily those of the NRC.

The NUREG series comprises (1) technical and administrative reports and books prepared by the staff (NUREG-XXXX) or agency contractors (NUREG/CR-XXXX), (2) proceedings of conferences (NUREG/CP-XXXX), (3) reports resulting from international agreements (NUREG/IA-XXXX), (4) brochures (NUREG/BR-XXXX), and (5) compilations of legal decisions and orders of the Commission and Atomic and Safety Licensing Boards and of Directors' decisions under Section 2.206 of NRC's regulations (NUREG-0750).

DISCLAIMER: This report was prepared as an account of work sponsored by an agency of the U.S. Government. Neither the U.S. Government nor any agency thereof, nor any employee, makes any warranty, expressed or implied, or assumes any legal liability or responsibility for any third party's use, or the results of such use, of any information, apparatus, product, or process disclosed in this publication, or represents that its use by such third party would not infringe privately owned rights.

NUREG/CR-6922
BNL-NUREG-77338-2006

P-CARES: Probabilistic Computer Analysis for Rapid Evaluation of Structures

Manuscript Completed: November 2006
Date Published: January 2007

Prepared by
J. Nie, J. Xu, and C. Costantino

Brookhaven National Laboratory
Upton, NY 11973-5000

V. Thomas, NRC Project Manager

Prepared for
Division of Fuel, Engineering and Radiological Research
Office of Nuclear Regulatory Research
U.S. Nuclear Regulatory Commission
Washington, DC 20555-0001
NRC Job Code N6103



ABSTRACT

Brookhaven National Laboratory undertook an effort to revise the CARES program under JCN N-6103. The revised CARES program (which is referred to as P-CARES in this report) includes many improvements over the existing CARES. A major improvement is the enhanced analysis capability in which a probabilistic algorithm has been implemented to perform the probabilistic site response and soil-structure interaction (SSI) analyses. This is accomplished using several sampling techniques such as the Latin Hypercube sampling (LHC), engineering LHC, the Fekete Point Set method, and also the traditional Monte Carlo simulation. This new feature enhances the site response and SSI analyses such that the effect of uncertainty in local site soil properties can now be quantified. Another major addition to P-CARES is a graphical user interface (GUI) which significantly improves the performance of P-CARES in terms of the inter-relations among different functions of the program, and facilitates the input/output processing and execution management. It also provides many user-friendly features that would allow an analyst to quickly develop insights from the analysis results.

This report describes the theoretical basis, probabilistic and deterministic site response and SSI analysis capabilities and many user-friendly features which have been implemented in P-CARES. Although the execution of P-CARES is driven by on-screen commands powered by the GUI and is self-explanatory, a user's guide is included in this report to serve either as a quick start or as a reference material for navigating through the program.

FOREWORD

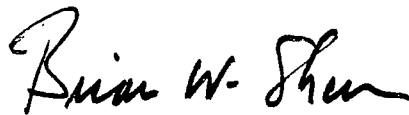
During the late 1980's, Brookhaven National Laboratory (BNL) developed the Computer Analysis for Rapid Evaluation of Structures (CARES) program under a Nuclear Regulatory Commission (NRC), Office of Nuclear Regulatory Research (RES) sponsored program. CARES was developed to provide the staff with a tool to evaluate the seismic response of relatively simple soil and structural models. BNL has completed an update to CARES by enhancing the analysis capability of the code to perform both deterministic and probabilistic site response and soil-structure interaction (SSI) analyses. In this report, the CARES code is referred to as probabilistic CARES (P-CARES).

This report describes the theoretical basis and analysis features for P-CARES, and contains a user's manual. The report also discusses the implementation of: (1) probabilistic algorithms in the code, using various sampling techniques such as Latin Hypercube (LHC) sampling, and traditional Monte-Carlo simulation, to perform probabilistic site response and soil-structure interaction (SSI) analyses; (2) a deterministic free-field response and SSI analyses; and (3) a post processing module, which provides various statistics on the simulation results.

Seismic response analyses involve the estimation of the effect of ground motions on structures at a particular site. The uncertainties inherent in ground motion and local site soil properties can be qualitatively considered in P-CARES, which uses a conservative deterministic analysis approach or probabilistic methods (in which uncertainties in earthquake size, location, and time of occurrence are explicitly considered).

The deterministic analysis approach of P-CARES has been validated/benchmarked by its application to a number of problems investigated by the NRC staff: (1) NUREG/CR-6896, "Assessment of Seismic Analysis Methodologies for Deeply Embedded NPP Structures," (2) NUREG-1750, "Assessment of Soil Amplification of Earthquake Ground Motion Using the CARES Code Version 1.2," and (3) NUREG/CR-6584, "Evaluation of the Hualien Quarter Scale Model Seismic Experiment." The probabilistic analysis approach used in P-CARES is based on the seismic probability risk assessment (PRA) method outlined in Appendix B of the American Nuclear Society (ANS) standard, "ANS/ANSI-58.21: External Events in Probabilistic Risk Assessment (PRA) Methodology."

With the development and implementation of these new features, including the addition of a graphical user interface (GUI) to improve the performance of the code, P-CARES provides a coherent approach to effectively perform evaluations of the seismic response of relatively simplified soil and structural models. It also gives the NRC staff the capability to perform a quick check and to carry out parameter variation studies of the SSI models and associated seismic data received from an applicant.



Brian W. Sheron, Director
Office of Nuclear Regulatory Research
U.S. Nuclear Regulatory Commission

TABLE OF CONTENTS

Abstract	iii
Foreword	v
List of Figures	xi
List of Tables.....	xv
Executive Summary	xvii
Acknowledgements	xxi
1 INTRODUCTION.....	1
1.1 Background.....	1
1.2 Scope and Objectives.....	2
1.3 Report Organization.....	3
2 THEORETICAL BASIS FOR P-CARES.....	5
2.1 Tools for Seismic Motion Processing.....	7
2.1.1 Arias Intensity.....	8
2.1.2 Lagrange Multiplier Based Accelerogram Correction.....	8
2.1.3 Fourier Transforms.....	10
2.1.4 Butterworth Filter.....	11
2.1.5 Fourier Components Smoothing.....	12
2.1.6 Response Spectrum.....	14
2.1.7 Power Spectral Density and Coherency.....	15
2.1.8 Time History Synthesis.....	16
2.2 Free-Field Analysis.....	18
2.3 Kinematic Interaction Algorithm.....	24
2.3.1 General Formulation.....	24
2.3.2 Free-field Solution and Shear Stress Evaluation.....	24
2.3.3 Best Fit.....	25
2.3.4 Determine Forces Acting on Foundation Area.....	26
2.3.5 Eliminate Forces on Foundation.....	27
2.4 Modeling of Structures and SSI.....	29
2.4.1 Description of the Model and Method of Solution.....	29
2.4.2 Mass Matrix.....	31
2.4.3 Damping Matrix.....	31
2.4.4 Stiffness Matrix.....	32
2.4.5 Forcing Functions.....	34
2.5 Probabilistic Simulation.....	36
2.5.1 Uncertainty Description.....	37
2.5.2 Fundamental Simulation Procedure.....	37
2.5.3 Simulation Schemes.....	38
2.5.4 Post Processing.....	41
3 SEISMIC ANALYSIS FEATURES OF P-CARES.....	43
3.1 Graphical User Interface.....	43

3.2	Seismic Motion Analysis	46
3.2.1	Accelerogram Convertor	46
3.2.2	Arias Intensity and Crop	47
3.2.3	Baseline Correction	47
3.2.4	Fourier Transforms	47
3.2.5	FC Processing	47
3.2.6	Response Spectra	48
3.2.7	PSD and Coherency	48
3.2.8	Time History Synthesis.....	48
3.3	Deterministic Free-Field Response and SSI Analysis	49
3.4	Probabilistic Free-Field Response and SSI Analysis	50
4	USER'S MANUAL DESCRIPTION	53
4.1	Short Tutorial	53
4.2	System Requirements	54
4.3	Components of P-CARES	55
4.3.1	Organization of Modules	56
4.3.2	Analysis Options.....	58
4.4	General Remarks on P-CARES Usage	60
4.4.1	File Name Conventions	60
4.4.2	File Name Input and File Browser.....	61
4.4.3	Toolbar and Menus	62
4.4.4	Plotting Toolbar	63
4.4.5	Progress Dialog.....	65
4.5	Seismic Motion Analysis	66
4.5.1	Accelerogram Convertor	66
4.5.2	Arias Intensity and Cropping.....	69
4.5.3	Baseline Correction	70
4.5.4	Fourier Transforms	71
4.5.5	FC Processing	72
4.5.6	Response Spectra	77
4.5.7	PSD and Coherency	78
4.5.8	Time History Synthesis.....	82
4.6	Site Response Analysis	85
4.6.1	General Information for Soil Column.....	86
4.6.2	Soil Layer Information	88
4.6.3	Correlation of Random Vector	90
4.6.4	Foundation for Kinematic Interaction.....	91
4.6.5	Site Response Calculation	93
4.7	SSI and Structural Analysis	94
4.7.1	Structural Modeling	95
4.7.2	Structural Response Calculation.....	100
4.8	Post Processing	105
4.8.1	Post Processing Interface	105
4.8.2	Post Processing Examples	106
5	SUMMARY	113

6	REFERENCES.....	115
Appendix A	Sample Problem	119
A.1	Synthetic Time History	119
A.2	Site Response Analysis.....	123
A.2.1	General Information.....	126
A.2.2	Soil Layer Information	127
A.2.3	Correlation	130
A.2.4	Foundation	130
A.2.5	Deterministic Site Response Analysis	131
A.2.6	Probabilistic Site Response Analysis.....	136
A.3	SSI and Structural Analysis	144
A.3.1	Nodes/Constraints.....	146
A.3.2	Beam.....	147
A.3.3	Damping	148
A.3.4	3D Model Viewer	148
A.3.5	Deterministic SSI and Structural Analysis	149
A.3.6	Probabilistic SSI and Structural Analysis.....	156

LIST OF FIGURES

Figure 2-1 Cumulative Arias Intensity Overlaid on Acceleration Record	8
Figure 2-2 Lagrange Multiplier Based Correction of Accelerogram	9
Figure 2-3 Application of Band Pass Butterworth Filter to A Fourier Spectrum.....	12
Figure 2-4 Application of Triangular Window Smoothing (Fixed-Width).....	13
Figure 2-5 Application of Triangular Window Smoothing (Varying Width)	14
Figure 2-6 Illustration of a Linear Oscillator.....	15
Figure 2-7 Soil Column and Rock Outcrop Motion	21
Figure 2-8 Illustration of Kinematic Interaction.....	28
Figure 2-9 Definition of Local Coordinate System for 3-D Beam.....	35
Figure 2-10 Simulation Concepts in P-CARES	36
Figure 2-11 A 2-D Latin Hypercube Sample	40
Figure 2-12 Comparison of 12 Fekete Points and LHC Points (Nie, 2003).....	41
Figure 2-13 Statistics of Response Spectra in Post Processing	42
Figure 3-1 P-CARES Splash Screen	44
Figure 3-2 P-CARES Main GUI	44
Figure 3-3 A Typical Console Panel Shown in the Main Display Panel.....	45
Figure 4-1 P-CARES Main GUI	54
Figure 4-2 P-CARES Component Layout.....	57
Figure 4-3 Subplot Configuration Dialog.....	64
Figure 4-4 An Annotated Accelerogram	65
Figure 4-5 A Progress Dialog For Probabilistic Simulation.....	66
Figure 4-6 After a High Pass Butterworth Filtering (low=0.2 Hz)	74
Figure 4-7 After a Low Pass Butterworth Filtering (High=10 Hz)	74
Figure 4-8 After a Band Pass Butterworth Filtering (Low=0.2 Hz, High=10 Hz).....	75
Figure 4-9 After Smoothing (fw=0.5 Hz) and Band Pass Filtering (Low = 0.2 Hz, High=10 Hz).....	75
Figure 4-10 After a Fixed Width Window Smoothing (fw=0.5 Hz)	76
Figure 4-11 After a Varying Width Window Smoothing (fw=20% f_c)	77
Figure 4-12 Example of Lagged Coherency.....	79
Figure 4-13 Example of Phase Spectrum	80
Figure 4-14 Example of Unlagged Coherency.....	80
Figure 4-15 Example of Arctanh Coherency.....	81
Figure 4-16 Site Response Analysis Interface.....	85
Figure 4-17 SSI and Structural Analysis Interface	95
Figure 4-18 Post Processing Example - Layer Thickness	107
Figure 4-19 Post Processing Example – Soil Weight Density	108
Figure 4-20 Post Processing Example – Soil Damping (Strain-Compatible).....	108
Figure 4-21 Post Processing Example – Low Strain Shear Modulus	109
Figure 4-22 Post Processing Example – Final Shear Modulus (Strain Compatible).....	109
Figure 4-23 Post Processing Example – Low Strain Shear Velocity	110
Figure 4-24 Post Processing Example – Final Shear Velocity (Strain Compatible).....	110
Figure 4-25 Post Processing Example – Statistics of Response Spectra	111
Figure 4-26 Post Processing Example – Statistics of Response Spectra With Input Motion.....	111
Figure A-1 Parameters for Time History Synthesis	120
Figure A-2 Design Spectrum Dialog for Reg. Guide 1.60	120
Figure A-3 The Synthetic Time History And Its Response Spectrum	121
Figure A-4 Synthetic Time History	122
Figure A-5 Fourier Spectra of the Synthetic Time History	122

Figure A-6 Soil Profile Used for Site Response Analysis (After Xu, et al 1990)	125
Figure A-7 Soil Profile Modeling - General Information.....	127
Figure A-8 Soil Profile Modeling - Soil Layer Information for Layer 1.....	128
Figure A-9 Soil Profile Modeling - Soil Layer Information for Layer 2.....	128
Figure A-10 Soil Profile Modeling - Soil Layer Information for Layer 3.....	129
Figure A-11 Soil Profile Modeling - Soil Layer Information for Layer 4.....	129
Figure A-12 Soil Profile Modeling - Correlation Definition.....	130
Figure A-13 Soil Profile Modeling – Foundation	131
Figure A-14 Calc Site Response - Deterministic Analysis.....	132
Figure A-15 Deterministic Site Response at 0 ft - Time History and Fourier Spectrum	132
Figure A-16 Deterministic Site Response at 10 ft - Time History and Fourier Spectrum	133
Figure A-17 Deterministic Site Response at 80 ft - Time History and Fourier Spectrum	133
Figure A-18 Deterministic Site Response at 120 ft - Time History and Fourier Spectrum	134
Figure A-19 Deterministic Site Response at 0 ft - Response Spectra	134
Figure A-20 Deterministic Site Response at 10 ft - Response Spectra	135
Figure A-21 Deterministic Site Response at 80 ft - Response Spectra	135
Figure A-22 Deterministic Site Response at 120 ft - Response Spectra	136
Figure A-23 Calc Site Response - Probabilistic Analysis	138
Figure A-24 Post Processing Tool for Simulation Results.....	138
Figure A-25 Probabilistic Soil Profile – Thickness.....	139
Figure A-26 Probabilistic Soil Profile – Weight Density.....	139
Figure A-27 Probabilistic Soil Profile – Damping	140
Figure A-28 Probabilistic Soil Profile – Low Strain Shear Velocity	140
Figure A-29 Probabilistic Soil Profile – Strain-compatible Shear Velocity.....	141
Figure A-30 Probabilistic Soil Profile – Low Strain Shear Moduli	141
Figure A-31 Probabilistic Soil Profile – Strain-compatible Shear Moduli.....	142
Figure A-32 Probabilistic Site Response Spectra - at 0 ft (Ground Surface)	142
Figure A-33 Probabilistic Site Response Spectra - at 10 ft below Ground Surface	143
Figure A-34 Probabilistic Site Response Spectra - at 80 ft below Ground Surface	143
Figure A-35 Probabilistic Site Response Spectra - at 120 ft below Ground Surface	144
Figure A-36 Stick Model of A Containment Structure for SSI Analysis [after Xu, et al, 1990]	145
Figure A-37 Structural Model - Nodes/Constraints	146
Figure A-38 Structural Model – Beam Definition.....	147
Figure A-39 Structural Model – Structural Damping.....	148
Figure A-40 Structural Model – 3D Structural Model Viewer	149
Figure A-41 Calc Structural Response – Joint SSI.....	150
Figure A-42 Deterministic SSI & Structural Analysis at Node 1 - Time History and Fourier Spectrum for the X Direction	151
Figure A-43 Deterministic SSI & Structural Analysis at Node 2 - Time History and Fourier Spectrum for the X Direction	151
Figure A-44 Deterministic SSI & Structural Analysis at Node 3 - Time History and Fourier Spectrum for the X Direction	152
Figure A-45 Deterministic SSI & Structural Analysis at Node 4 - Time History and Fourier Spectrum for the X Direction	152
Figure A-46 Deterministic SSI & Structural Analysis at Node 5 - Time History and Fourier Spectrum for the X Direction	153
Figure A-47 Deterministic SSI & Structural Analysis at Node 1 - Response Spectra the X Direction.....	153
Figure A-48 Deterministic SSI & Structural Analysis at Node 2 – Response Spectra for the X Direction.....	154

Figure A-49 Deterministic SSI & Structural Analysis at Node 3 – Response Spectra for the X Direction	154
Figure A-50 Deterministic SSI & Structural Analysis at Node 4 – Response Spectra for the X Direction	155
Figure A-51 Deterministic SSI & Structural Analysis at Node 5 – Response Spectra for the X Direction	155
Figure A-52 Probabilistic Structural Response Spectra - For X Direction at Node 1	156
Figure A-53 Probabilistic Structural Response Spectra - For X Direction at Node 2	157
Figure A-54 Probabilistic Structural Response Spectra - For X Direction at Node 3	157
Figure A-55 Probabilistic Structural Response Spectra - For X Direction at Node 4	158
Figure A-56 Probabilistic Structural Response Spectra - For X Direction at Node 5	158

LIST OF TABLES

Table 2-1 Soil Degradation Models	22
Table A.1 Low-strain Soil Properties.....	126
Table A.2 Distribution Parameters for Soil Layer Properties.....	126
Table A.3 Strain-compatible Soil Profile	136

EXECUTIVE SUMMARY

In the process of review and evaluation of nuclear power plant (NPP) structure designs, it is essential to understand the behavior of seismic loading, soil condition, foundation, and structural properties and their impact on the overall structural response. During the late 1980's, Brookhaven National Laboratory (BNL) developed the CARES (Computer Analysis for Rapid Evaluation of Structures) program for the United States Nuclear Regulatory Commission (NRC). CARES was intended to provide the NRC staff with a coherent approach to effectively perform evaluations of the seismic response of relatively simplified soil and structural models. Such an approach provides the NRC staff with a capability to quickly check the validity and/or accuracy of the soil-structure interaction (SSI) models and associated data received from various applicants. These submittals are typically obtained from numerical studies performed with large state-of-the-art structural computer packages which are difficult to assess without spending a significant amount of time and effort in the review process. By performing simplified model studies, the sensitivity of computed responses to variations in a host of controlling parameters can often be evaluated and thereby assist the staff in gaining confidence in the results obtained from the larger computer studies.

The initial version (Version 1.0, Xu et al. 1990) of the CARES program was developed by combining two available computer programs which treat the free-field response calculation (the SLAVE Code, Costantino and Miller, 1979) and the soil-structure interaction analysis of simplified stick models (the SIM Code, Miller and Costantino, 1979) to perform simplified deterministic site response and SSI analyses. Three later revisions had been made to CARES, namely CARES v.1.1 (Costantino et al., 1992), CARES v.1.2 (Costantino et al., 1995), and CARES v. 1.3 (Miller and Costantino, 2000).

The current revision, which is described in this report, was undertaken by BNL during FYs 2005 and 2006 in the NRC program under JCN N-6103. The NRC Project Manager was Mr. Vaughn Thomas and the BNL Principal Investigator was Dr. Jim Xu. The program development was performed by Drs. Jinsuo Nie, Jim Xu, and Carl Costantino. The primary objective of this program was to enhance the analysis capability by implementing a probabilistic algorithm in CARES (Probabilistic CARES, to be referred to hereafter in this report as P-CARES) to perform the probabilistic site response and SSI analyses. This was accomplished using various sampling techniques such as the Latin Hypercube sampling (LHC), engineering LHC, the Fekete Point Set method, and also the traditional Monte Carlo simulation. The deterministic capability of P-CARES was also improved with add-on features using the graphical user interface (GUI). The resulting probabilistic P-CARES treats the low-strain soil properties as random variables and applies any of the four sampling techniques to generate random soil columns. These random columns are used for convolution analysis, which in turn provide input for the SSI response analysis. By implementing the sampling process, the effect of the uncertainty inherent in the low-strain soil properties is propagated through the site and SSI responses. The results of the probabilistic SSI analysis are expressed in terms of the median, mean, and various percentiles in the free field response and the in-structure response spectra.

The deterministic analysis approach of P-CARES has been validated/benchmarked by its application to a number of problems investigated by the NRC staff: (1) NUREG/CR-6896, "Assessment of Seismic Analysis Methodologies for Deeply Embedded NPP Structures," (2) NUREG-1750, "Assessment of Soil Amplification of Earthquake Ground Motion Using the CARES Code Version 1.2," and (3) NUREG/CR-6584, "Evaluation of the Hualien Quarter Scale Model Seismic Experiment." The probabilistic analysis approach used in P-CARES is based on

the seismic probability risk assessment (PRA) method outlined in Appendix B of the American Nuclear Society (ANS) standard, "ANS/ANSI-58.21: External Events in Probabilistic Risk Assessment (PRA) Methodology."

P-CARES is intended to be used by persons with practical experience in seismic design and analysis of nuclear power plants and other structures, estimation of earthquake ground motion, and seismic probabilistic risk assessment. The P-CARES code can perform a site response and SSI analyses where the soil profile is limited to horizontal layers and the structure is reasonably approximated by lumped mass beam systems. However, the site response analysis of P-CARES can be extended to a site with the topographical features (inclined soil layers). In this case, several base profiles need to be identified to represent the site in a bounding fashion, and for each base profile, the probabilistic site response analysis is performed, and the results for all of base profiles are then combined to obtain the site response.

In addition, the existing CARES, albeit user-friendly in a DOS world more than a decade ago, lacks a GUI that can greatly improve usability and productivity. GUI programming is now relatively easy to achieve due to the advances in computer technology. Therefore, as part of this project, a GUI was added to P-CARES to facilitate the input/output processing and execution management.

The existing CARES Version 1.3 has been upgraded to FORTRAN 90/95 to add clear interfaces between subroutines that are necessitated by the probabilistic simulation, to remove many input/output states that are not suitable for simulation, and to take advantage of the dynamic memory allocation for problem size, to improve the logic and the code quality, among many other improvements. The upgraded version of CARES becomes a few compiled modules that are accessed in Python, and constitutes the computational core in the P-CARES. Building around this computational core, probabilistic simulation and a GUI have been developed to form the integrated software package. The software architecture of P-CARES follows the object-oriented approach, the current state-of-the-art programming technique, which enables it to be very flexible and, therefore, can be modified for future upgrades. A rapid application development aspect of P-CARES utilizes the strategy of mixed programming in Python and FORTRAN, with Python serving as a powerful glue language while FORTRAN is used for the computational core involving heavy number crunching.

P-CARES provides the capabilities to perform deterministic and probabilistic site response and soil-structure interaction (SSI) analyses based on relatively simplified soil and structural models. It automatically manages data and calculations in the probabilistic simulation with any arbitrary number of samples. The sample soil profiles and the response spectra of the simulated soil and structural responses can be aggregated statistically in terms of mean, median, and different percentiles curves. These statistical measures may provide more valuable insights and inferences than those in deterministic soil and structural analysis, in the process of review and evaluation of nuclear power plant (NPP) structure designs. The probabilistic analysis capability in P-CARES becomes especially important as the nuclear industry is more widely accepting the probabilistic approach to account for the uncertainties inherent in the natural and built environments.

P-CARES also provides a set of utility functions for seismic motion analysis, which include the Arias Intensity calculation, accelerogram manipulation, Fast Fourier Transformation and its inverse, baseline correction of accelerograms, Butterworth low pass / high pass / band pass filtering, window smoothing, response spectrum generation, power spectrum density and coherency generation, and time history synthesis. The utility functions can be used to preprocess an accelerogram for the site response and SSI analysis, and can also be used for post processing

for deterministic analysis. Another well-suitable application of these utilities is to simply examine the characteristics of a given accelerogram.

The P-CARES GUI integrates all the above-mentioned functions in one package, instead of a few stand-alone programs in the traditional CARES. It provides convenient on-screen model building capability for soil and structural models, automatic analysis management, and intuitive feedback of instant display of figures. The generated figures can be saved in various popular image formats or in data files that can be readily imported into any spreadsheet programs such as Excel for further processing. Also, it greatly improves the productivity and makes P-CARES a valuable tool to assist the staff in evaluation of the site and structural analysis data submitted by the applicants.

ACKNOWLEDGEMENTS

This report was prepared as part of a research program sponsored by the Office of Nuclear Regulatory Research of the U.S. Nuclear Regulatory Commission. The authors would like to express their gratitude to Mr. Vaughn Thomas, NRC Project Manager, for his encouragement, and the technical and administrative support he has provided throughout the course of this project.

The authors would like to express their appreciation to Mr. Herman Graves (NRC), Dr. Anthony Hsia (NRC), and Dr. Charles Hofmayer (BNL) for their continued support throughout the development of CARES, especially the support and technical suggestions they provided for this major revision.

The development of CARES would not be possible without the dedicated effort of Dr. Charles A. Miller who passed away during the preparation phase of this project. The authors wish to express their appreciation to Dr. Miller for his contribution and advice which led to the successful completion of this project.

The authors also wish to express special thanks to Ms. Susan Monteleone for her secretarial help in the preparation of this report, especially for providing her "Happy Nuke" picture used in the splash screen for P-CARES.

1 INTRODUCTION

1.1 Background

In the process of review and evaluation of nuclear power plant (NPP) structure designs, it is essential to understand the behavior of seismic loading, soil condition, foundation, and structural properties and their impact on the overall structural response. During the late 1980's, Brookhaven National Laboratory (BNL) developed the CARES (Computer Analysis for Rapid Evaluation of Structures) program for the United States Nuclear Regulatory Commission (NRC). CARES was intended to provide the NRC staff with a coherent approach to effectively perform evaluations of the seismic response of relatively simplified soil and structural models. Such an approach provides the NRC staff with a capability to quickly check the validity and/or accuracy of the soil-structure interaction (SSI) models and associated data received from various applicants. These submittals are typically obtained from numerical studies performed with large state-of-the-art structural computer packages which are difficult to assess without spending a significant amount of time and effort in the review process. By performing simplified model studies, the sensitivity of computed responses to variations in a host of controlling parameters can often be evaluated and thereby assist the Staff in gaining confidence in the results obtained from the larger computer studies.

The initial version (Version 1.0, Xu et al. 1990) of the CARES program was developed by combining two available computer programs which treat the free-field response calculation (the SLAVE Code, Costantino and Miller, 1979) and the soil-structure interaction analysis of simplified stick models (the SIM Code, Miller and Costantino, 1979) to perform simplified deterministic site response and SSI analyses. Desirable ancillary pre- and post- processing capabilities were added (developing models, plotting, spectra and PSD computation, etc.) to enhance the usefulness of the program. The CARES program is designed to operate in a desktop PC environment (either DOS or Macintosh systems). It is geared to provide user friendly input/output features with rapid turnaround. The primary functions of CARES 1.0 included:

- + A free-field computational algorithm allows for analysis of the seismic response of a layered soil column subjected to upwardly propagating horizontal shear waves developed by a given input seismic motion. The input motion can be specified by means of a target response spectrum appropriate for a given earthquake magnitude at a given range from the source, or an actual accelerogram at a given location within the soil column. The output from this computation is the motion at other locations within the soil column which is compatible with this input motion as well as the final stress and strain conditions developed in each soil layer.
- + A structural response calculation generates the seismic response of a structure embedded within or on the soil resulting from the ground motions generated in the free-field module above. This calculation includes the effects of depth of burial on the SSI impedance functions used in the structural response calculation.
- + A variety of pre- and post- processing capabilities.

Since the original development, the usefulness of CARES has been validated by its application to a number of problems investigated by the NRC staff. Having the capability to easily perform small analyses directly on a PC has been shown to be a valuable asset for the Staff, which also led to the continued improvement of CARES over the years. To this end, three revisions have been

made to CARES, namely, CARES v.1.1 (Costantino et al., 1992), CARES v.1.2 (Costantino et al., 1995), and CARES v. 1.3 (Miller and Costantino, 2000). The following is a brief description of the modifications included within each of the revisions:

Version 1.1 - The main changes in Version 1.1 had the objective of increasing the size of problems that could be treated with CARES. This required a rearrangement of the storage arrays in the structural response portion of the code and the inclusion of an improved Fast Fourier Transform to reduce the running times for large problems. Several changes were made to the soils portion of CARES which extends the capability of the program. The first change allowed for the inclusion of a rock outcrop model within the soil column formulation. Extended soil degradation modules were also incorporated to keep pace with new developments.

Version 1.2 - The second enhancement to the Code was undertaken to enable it to run on the Sun SPARC workstation, located at NRC, which operates in the UNIX environment. A number of additions were also made to extend the capabilities of the analysis. In the structural module, several aspects have been modified. The capability for treatment of rigid links within the structural model, an improved algorithm for handling composite damping, and an in-plane shear wall element, were added to the Code. The SSI portion of the Code was also modified to include rectangular foundations.

Version 1.3 - The essential changes associated with this revision are the addition of kinematic interaction effects, and the improvement of the damping models available for the structural analysis.

With the computing power increasing at the exponential rate in recent years, the demand for better and accurate characterization of the effect of earthquake ground motions on the site and SSI structural responses also led to the development of many state-of-the-art analytical methods. These advanced methods employ the random vibration theory or large-scale simulation algorithms to treat the stochastic seismic response with probability theories. As a result, the effort required for performing probabilistic analyses becomes far more complicated than that required for a deterministic analysis. Furthermore, the interpretation of the results from a probabilistic analysis becomes more subtle and less straightforward than the traditional deterministic analysis.

To meet the need for an efficient and effective tool to perform site response and SSI analyses in the probabilistic space, a major revision to CARES is made under JCN N-6103 to incorporate the probabilistic capability and a graphical user interface (GUI) into the program. The objective of this report is to provide a description of the improved capabilities of CARES and a user's guide.

1.2 Scope and Objectives

It is generally recognized that large uncertainty exists in seismic response analyses of structures. The uncertainty arises mainly from the limited understanding of the seismic sources, attenuation relations, local site soil effect, and structural properties. The current procedure for quantifying the uncertainty in seismic response analyses is to use deterministic bounding approaches such as those outlined in Standard Review Plan (SRP) 3.7 (NUREG-0800, 1989) and ASCE 4-98 (1998), which are widely viewed as being conservative. Recent advances in the stochastic seismic analysis have shown that a more accurate prediction of the seismic response considering uncertainty can be obtained by resorting to the probabilistic procedure. The scope of the current revision aims at implementing the probabilistic procedure in both site response and SSI analyses of CARES, to be referred hereinafter as P-CARES (probabilistic CARES).

The probabilistic site response and SSI analysis is the state-of-the-art seismic analysis approach which is gaining wider acceptance by the nuclear industry. Recently published ASCE 43-05 (2005) has opted for the probabilistic approach for determining the design factor for soil site, given a rock input motion. ANS External Event PRA Methodology Standard (ANSI/ANS-58.21, 2003) went a step further to require a probabilistic SSI response analysis for a complete-scope seismic probabilistic risk assessment (SPRA). Included in the scope for P-CARES is to provide the NRC staff with an important tool for evaluating and verifying the probabilistic site response and SSI analyses performed by licensees. However, the level of uncertainty to be addressed in P-CARES will be limited to local site soil effects. The uncertainty in structural properties, e.g., the lumped masses and the Young's moduli, is relatively small compared to other sources of uncertainty, and could be neglected without loss of much accuracy in SSI analyses. Uncertainty in ground motions is probably the largest among all sources considered. The ground motion uncertainty can be addressed using a similar approach to the way the soil uncertainty is addressed in P-CARES. However, the implementation of a probabilistic procedure to capture the uncertainty in ground motions requires the development of a ground motion database binned in terms of magnitude and distance in a manner that allows for extending the probabilistic simulation to the ground motion database. Since the development of a complete ground motion database could require sizeable effort, it is, therefore, beyond the scope of the current P-CARES development; however, it could be considered as a future improvement to the program.

The primary objective of this program under JCN N-6103 is to enhance the analysis capability by implementing a probabilistic algorithm in P-CARES to perform the probabilistic site response and SSI analyses. This is accomplished using various sampling techniques such as the Latin Hypercube sampling (LHC), engineering LHC, the Fekete Point Set method, and also the traditional Monte Carlo simulation. The deterministic capability of P-CARES will also be improved with add-on features using GUI. The resulting probabilistic P-CARES will treat the low-strain soil properties as random variables and applies any of the four sampling techniques to generate random soil columns. These random columns will then be used for convolution analysis, which in turn will provide input for the SSI response analysis. By implementing the sampling process, the effect of the uncertainty inherent in the low-strain soil properties is propagated through the site and SSI responses. The results of the probabilistic SSI analysis are expressed in terms of the median, mean, and various percentiles in the free field response and the in-structure response spectra.

In addition, the existing CARES, albeit user-friendly in a DOS world a decade ago, lacks a GUI that can greatly improve usability and productivity. GUI programming is now relatively easy to achieve due to the advances in computer technology. Therefore, the second goal of this project is to add a GUI to P-CARES that facilitates the input/output processing and execution management.

P-CARES will provide the NRC staff with the capability to effectively evaluate the probabilistic seismic response using simplified soil and structural models and to quickly check the validity and/or accuracy of the SSI data received from applicants and licensees.

1.3 Report Organization

This report consists of six sections. Following this introduction section, Section 2 describes the theoretical basis for various components in P-CARES, which include a number of seismic motion processing utilities, free field convolution analysis, foundation kinematic interaction, structural response analysis, and the probabilistic simulation algorithms. The emphasis in this section is on providing a description of the underlying theories used in P-CARES rather than a complete derivation of the theory for the sake of conciseness. Section 3 presents the P-CARES features for seismic site response and SSI analyses and the associated seismic motion utilities. It also

discusses the software development tactics and the graphical user interfaces. This section serves as an overview of the P-CARES program and its various application scenarios. Section 4 provides a detailed user's manual that describes aspects of P-CARES down to every button in the GUI. It includes a short tutorial to help the user with a first view of the program, system requirements for a complete list of software packages that P-CARES uses, a description of P-CARES design architecture and the usage options, and a detailed description for each of the interfaces used in various analysis scenarios. Section 5 concludes this report with a summary of the P-CARES development and seismic analysis features. The last section provides a complete list of the references. An appendix at the end of this report provides an example that demonstrates the use of the time history synthesis tool, the deterministic and probabilistic site response analyses, and the deterministic and probabilistic SSI and structural analyses.

2 THEORETICAL BASIS FOR P-CARES

This section provides the theoretical basis for P-CARES. The primary objective of the P-CARES program is to perform both deterministic and probabilistic site response and soil-structural interaction (SSI) analyses based on simplified models for soil columns and structures. Useful features associated with processing ground motions are also included in P-CARES. Although the implementation and outputs required for the deterministic and probabilistic analyses are different, these two types of calculation are considered to be similar due to the fact that the deterministic analysis simply corresponds to one sample calculation in the simulation performed in the probabilistic analysis. Therefore, the theoretical bases common to both calculations are described in this section, which include: 1) free-field convolution analysis; 2) kinematic interaction analysis, and 3) structural response analysis including the SSI effect. The probabilistic simulation is described in the context of the site response analysis with assumed variabilities in soil properties and their effect on the structural response through SSI. The theoretical basis for the sampling techniques implemented in P-CARES is also described.

For the deterministic analysis or one sample analysis in the simulation, the soil is idealized as a horizontally stratified system and is modeled as a one-dimensional (1-D) shear beam while the structure is modeled as 3-D lumped-mass elastic system. The free-field response calculation is carried out using the frequency domain time history analysis. The structural response can be calculated separately in each of the three directions or for all directions simultaneously to account for torsional effects. The latter is only feasible in a deterministic SSI analysis of structures. The response of the structure (time histories or spectral representations of the time histories at selected locations) including the SSI effect is evaluated, given a seismic input motion or the free-field response. Since the computations are performed in the frequency domain, Fast Fourier Transforms (FFT) are utilized to obtain the time domain responses.

For the probabilistic simulation analysis, seismic input motion and structural properties are considered deterministic, even though they can exhibit great variability especially for seismic input motion. Variability in seismic input motion is largely attributed to the characteristics of seismic sources and attenuation relations, and can be determined by a simulation analysis drawing from a database of ground motions binned in terms of earthquake magnitude and distance. The current version of P-CARES does not consider the variability in seismic input motion; however, such variability can be incorporated into P-CARES by developing a ground motion database. Since nuclear power plant (NPP) structures are generally constructed through controlled processes, variability in structural properties is much smaller than respective variability in ground motions and soil properties, and therefore, is neglected in P-CARES. The probabilistic analysis in P-CARES emphasizes on the effect of variability in local soil properties. Soil layer thickness, soil density and soil shear modulus are modeled by lognormal random variables with correlation enabled. The fundamental scheme of the probabilistic analysis is: given a specified seismic input, the site responses and structural responses are calculated with the uncertainties of the soil column propagating to the structures.

The underlying theories of P-CARES can be grouped into five interconnected and distinguishable modules. Each of these is briefly described below, and is followed by more detailed discussions of the methods used in P-CARES.

Seismic Motion Analysis - This module is a collection of utility routines that process seismic accelerograms and their Fourier components. It can be used to preprocess raw seismic records, to generate synthetic time histories for given target response spectra, or to post-process the responses from free-field analysis and structural analysis. The utilities include: 1) raw

accelerogram conversion, 2) Arias Intensity calculation, 3) accelerogram cropping, 4) baseline correction to reduce residual velocity and displacement, 5) Fast Fourier Transformation (FFT) and the inverse FFT, 6) Butterworth filter for Fourier Spectra, 7) window smoothing for Fourier Spectra, 8) response spectra, 9) auto Power Spectrum Density (PSD) and coherency calculations, and 10) time history synthesis. All these utilities allow for graphical displays of relevant information for on-screen visual feedback, output in various image format, and data in text format.

Free-Field Convolution Analysis - This module performs the free-field response analysis, based on a simplified 1-D horizontally stratified soil column model. For each layer of the soil column, the user can specify the soil properties such as: the mass density, low-strain shear velocity, layer thickness, and its degradation model which provides strain-compatible shear modulus and damping value for each layer. The mass density, low-strain shear velocity and the layer thickness also require the means and the standard deviations to define the random variable distributions if a probabilistic analysis is to be performed. Correlations between these random variables can also be specified. The input motion, which needs to be transformed into Fourier components for convolution analysis, can be specified at the ground surface, rock outcrop, or the bottom of any soil layer. In situations where only accelerograms or criterion response spectra are available, the user can generate the Fourier components using the seismic motion analysis module described above. The computational model of the 1-D layered soil column in P-CARES assumes vertical propagation of horizontally polarized shear waves and uses standard convolution methods. Degradation effects can be included in the soil by an iterative elastic solution method, in which the iteration process stops until the degraded soil properties are compatible with the strain levels for the given input motion. The user can request locations where free-field output motions are needed. For kinematic SSI problems, the motions required at depths over the embedment are automatically generated for a prescribed number of depths and these depths are evenly distributed over the embedment depth. All output motions are represented by Fourier components.

Kinematic Interaction Analysis - This module computes the translational and rocking responses of an embedded foundation to the free-field input motion. The foundation is assumed rigid and massless for the purpose of kinematic interaction analysis. For surface foundations, since kinematic interaction effect does not exist for 1-D layered soil column, this analysis is not required. In contrast with the multilayered soil column model in previous module, the soil is represented in this module as two layers: one to the side of the foundation and one beneath the foundation. This restriction is required to obtain an efficient analytical solution because the foundation impedance functions are only available for such simple soil system. This simplified model has been adopted in P-CARES to avoid a coupled soil-structure interaction solution that requires the use of a complex code such as SASSI. The user needs to select the type and the dimension of the foundation, and specifies the soil properties on the side and under the base of the foundation. However, the user can also simply provide a soil profile and let P-CARES to calculate the side and base soil properties based on certain weighted averaging rules. The free-field motions computed in the previous module at depths distributed over the embedment depth of the foundation are used as input to compute the response of the foundation. The translational and the rocking motions of the foundation are assumed as displacements at the basemat level. The resulting motions are evaluated by first obtaining a best rigid body displacement fit to the input free-field accelerograms and then applying additional displacements eliminating the free-field stresses induced due to the imposed rigid body displacements at the foundation soil interface. The resulting motions are saved as Fourier components and are used as the input motions to structural analysis module.

The kinematic interaction analysis is integrated in the free-field analysis module. This integration provides a convenient approach to automatically generate the output motions over the embedment depth for the kinematic analysis.

Structural Analysis - This module evaluates the response of the structure to the input motions. The structure model is a lumped mass system connected with elastic elements and constrained with a SSI node. The elements can be elastic beam elements and shear wall elements, and the special rigid links. The SSI node is the location where the input motions are applied and is modeled by a two-layer soil system similar to that in the kinematic analysis module. The input motions in the structural analysis module can be any combination of the three translational and three rotational components; however only two are available if the motions are generated from the previous free-field and kinematic analyses. If the structure sits on a surface foundation, the input motions can only be translational and there is not kinematic interaction effect involved. The outputs are the Fourier components of the accelerograms at selected nodal locations within the structure.

Probabilistic Simulation – This module provides P-CARES the capability to generate correlated random vectors, to carry out the deterministic analysis for each sample, and to manage various simulation outputs. This module is placed on top of the free-field convolution analysis, kinematic SSI analysis, and the structural analysis, and streamlines these analyses with the number of samples specified by the user. The random vector includes the soil layer thickness, soil density, and the low-strain soil shear modulus, and is expandable to include other properties. All random variables are modeled as log-normal variables. The user can specify the number of random variables (currently a function of the number of soil layers) and the number of samples in the simulation. In this module, the uncertainties inherent in the soil column randomly filter the input seismic motion and propagate through the site and SSI responses. The simulation results can then be aggregated by statistical means of median, mean, and various percentiles in the post processing module. The simulation schemes implemented in this module include the Monte Carlo simulation, Latin HyperCube sampling (LHC), engineering LHC, and the experimental Fekete Point Set method.

2.1 Tools for Seismic Motion Processing

This subsection presents a summary of the utility algorithms implemented in P-CARES to process seismic or response motions, which are discrete series in time or frequency domains. The implemented algorithms are Arias Intensity calculation, baseline correction, Fast Fourier Transformation (FFT) and the inverse FFT, Butterworth filter for Fourier Spectra, Window smoothing for Fourier Spectra, Power Spectrum Density, and Time History Synthesis. Most of these algorithms operate in the frequency domain; therefore the FFT and its inverse are the essential algorithms. The basic assumption for Discrete Fourier Transform (DFT) is that the seismic and response motions are periodic functions in the time domain with the period equal to the duration of the motions. This assumption can be expressed as:

$$a(t) = \sum_{j=0}^{m-1} A_j e^{i\omega_j t} \quad (2-1)$$

where m is the total number of frequency components of the motion (including the zero or steady state term) equally spaced at a constant frequency increment, ω_j is the circular frequency, and A_j is the complex Fourier coefficient of the sinusoidal motion.

2.1.1 Arias Intensity

As the peak ground acceleration (PGA) is not an ideal measure of the intensity of the earthquake, Arias Intensity (Arias, 1970) has been introduced to measure the energy content of the earthquake. It is defined as,

$$I_{Arias} = \frac{\pi}{2g} \int_0^T a(t)^2 dt \quad (2-2)$$

where g is the gravity acceleration, T is the duration of the ground acceleration record, and the Arias Intensity I_{Arias} is in the unit of length/time. Figure 2-1 shows a typical acceleration record with its cumulative Arias Intensity overlaid on it. This figure also shows several time locations, e.g. T05 and T75 in the figure, when the cumulative energies are at the related percentile. Arias Intensity has been often used to define the strong ground motion, the duration of which covers from 5% to 75% of the total cumulative energy (ASCE/SEI 43-05). Although this definition of the strong ground motion has been widely accepted, it does not necessarily capture all the characteristics of the motion. The strong motion duration is defined by,

$$T_{sm} = T75 - T05. \quad (2-3)$$

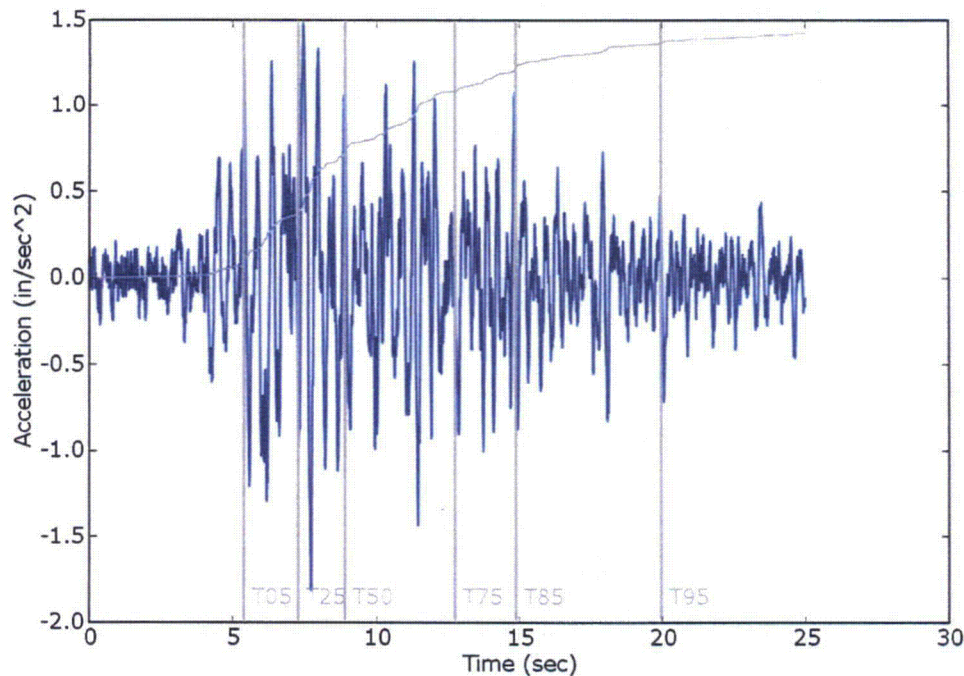


Figure 2-1 Cumulative Arias Intensity Overlaid on Acceleration Record

2.1.2 Lagrange Multiplier Based Accelerogram Correction

Measured and synthesized acceleration records usually have nonzero residual velocity and displacement that appear unrealistic. Even though permanent displacements, due to nonlinear soil deformation, are typically observed after a strong earthquake, a recorded accelerogram applied in analysis very often do not reproduce this permanent displacement correctly, for reasons such that the accelerogram may be cropped for efficiency in the application. In addition, these nonzero residual velocity and displacement often do not impose a serious influence to analyses in which the base shift does not affect the analytical responses, such as relative displacement and forces. In this regard, the removal of these nonzero residual velocity and displacement from an

accelerogram appears of little importance; on the other hand, purposely keeping them in an accelerogram is not necessary for many applications. However, in some other situations, such as simultaneously applying multiple seismic inputs at different locations in a structure or consecutively applying motions to a structure to simulate multiple earthquake events, the residual velocity and displacement may have a significant impact on the solution and may need to be removed. There are a number of methods in the literature to correct the accelerogram (e.g. Jennings et al, 1968), this utility in P-CARES adopts a Lagrange multiplier based method that was developed by Borsoi and Richard (1985).

This method requires an accelerogram be discretized evenly in time. The principle of this method is to solve a minimization problem of a quadratic form with linear constraints by the Lagrange multiplier method, where the quadratic form is the Euclidean norm between the corrected and uncorrected accelerograms, and the linear constraints are for zeroing out the final velocity, the final displacement, and the average displacement that are expressed in linear combinations of the accelerogram. The minimization in the method ensures a minimal modification to the original accelerogram. There are different ways to obtain the linear constraints as linear combinations of the accelerogram, adopted in this utility is the simple and effective method in Borsoi and Richard (1985), which assumes linearity between nearby data points in the accelerogram, velocity and displacement records. These assumptions are not compatible because a linear assumption in acceleration implies parabolic relation in velocity and cubic relation in displacement. However, these assumptions do not affect much the effectiveness of the correction if the time increment is sufficiently small, which is true for most accelerograms in practice.

Figure 2-2 shows an example of using this utility to correct a sample accelerogram, where the dotted red curves are for the uncorrected accelerogram while the solid blue curves are after the correction. It shows that the modification to the original accelerogram is indistinguishable, while the corrections to the velocity and the displacement are significant. It also indicates that the correction mainly affects the low frequency components.

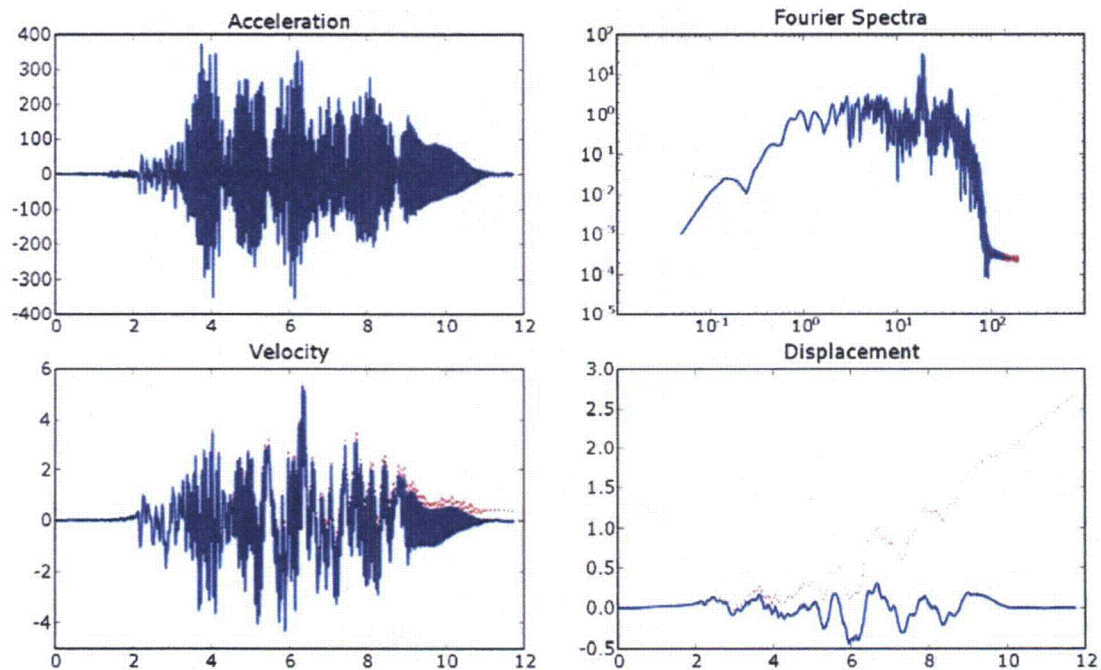


Figure 2-2 Lagrange Multiplier Based Correction of Accelerogram

2.1.3 Fourier Transforms

In earthquake engineering, the acceleration $a(t)$ is digitalized or recorded as a series of acceleration values with constant time intervals. Let the acceleration sequence be designated as $\{a_i, i = 0, \dots, N-1\}$, where N is the number of the data points in the earthquake record, then the time interval can be expressed in terms of the total duration T as:

$$\Delta t = T / N \quad (2-4)$$

The forward DFT is defined by:

$$A_k = \frac{1}{N} \sum_{j=0}^{N-1} a_j e^{-i2\pi jk/N} \quad \text{for } k = 0 \dots N-1, \quad (2-5)$$

and the inverse DFT is:

$$a_j = \sum_{k=0}^{N-1} A_k e^{i2\pi jk/N} \quad \text{for } j = 0 \dots N-1. \quad (2-6)$$

The above definitions of forward and inverse Fourier transforms are different than the most common ones that the denominator of N does not appear in the forward DFT but in the inverse DFT. These two different approaches to the Fourier transform couple definition yield the same accelerograms but different Fourier components. This particular implementation in P-CARES is for efficiency considerations due to many inverse DFTs are involved in the convolution analysis. Direct application of DFT in practice for large records can take considerable time, which is proportional to N^2 . A much faster algorithm was developed by Cooley and Tukey (1965), and has been denoted as Fast Fourier Transform (FFT). The FFT implemented in P-CARES is similar to the original Cooley and Tukey algorithms, and has a time bound of $N \log_2 N$. It is required in this algorithm that the number of data in a record to be a power of 2, i.e.,

$$N = 2^M, \quad (2-7)$$

where M is a positive integer, and usually takes the smallest integer that makes 2^M be equal to or greater than the number of data points in the available record. The acceleration record is extended by padding zeros at the end of the record to meet this requirement.

While the FFT algorithm used in P-CARES (Equation 2-5) requires the total number of Fourier components is the same as the number of time points, the particular formulation used requires only one-half the number of coefficients, with the remaining determined as the complex conjugates. In another words, Fourier components $0 \dots N/2$ sufficiently represent the frequency content of the whole acceleration record of N data points. The number of independent Fourier coefficients is given by,

$$N_c = N/2 + 1. \quad (2-8)$$

The corresponding frequency increment and the maximum frequency content of the acceleration, i.e., the Nyquist frequency, can be determined from,

$$\Delta f = 1/T, \quad (2-9)$$

$$f_{\max} = 1/2\Delta t \quad (2-10)$$

For example, if the total acceleration duration is 20 seconds and the parameter M in Equation 2-7 is selected as 11, the characteristics of the acceleration record and its Fourier components by FFT are determined in the following,

T	= 20 seconds	N	= 2048 data points
Δt	= 0.00977 seconds	N_C	= 1025 frequency records
Δf	= 0.05 hz	f_{\max}	= 51.20 hz

2.1.4 Butterworth Filter

The low pass filter implemented in P-CARES is a Butterworth filter (Butterworth, 1930) of an order 4. The general transfer function of a Butterworth filter is defined as (Proakis and Manolakis, 1988),

$$|H(\omega)|^2 = \frac{1}{1 + (\omega/\omega_l)^{2N}}, \quad (2-11)$$

where ω_l is the low pass cutoff frequency and N is the order of the filter. A higher order Butterworth filter ramps the frequency response faster to zero.

The high pass filter implemented in P-CARES is a modified version of the regular low pass Butterworth filter:

$$|H(\omega)|^2 = \frac{1}{1 + (\omega_h/\omega)^{2N}}, \quad (2-12)$$

where ω_h is the high pass cutoff frequency and $N = 4$ in the particular implementation in P-CARES. The above equation applies only for $|H(\omega)| \geq 0.5$; otherwise, a truncated linear format is used as follows,

$$|H(\omega)| = \max(0, 0.5 - C(\omega_{05} - \omega)) \quad (2-13)$$

where ω_{05} is the frequency such that $|H(\omega)| = 0.5$ in Equation 2-12, and C is a constant defined as,

$$C = \frac{4}{\omega_h} \left(\frac{\omega_h}{\omega_{05}} \right)^9 \left/ \left(1 + \left(\frac{\omega_h}{\omega_{05}} \right)^8 \right)^{3/2} \right. \quad (2-14)$$

The high pass and low pass Butterworth filters can be applied in series to form a band pass filter. To obtain a filtered Fourier spectrum $F'(\omega)$, a selected filter $H(\omega)$ is applied to the original Fourier spectrum $F(\omega)$ as follows,

$$F'(\omega) = H(\omega)F(\omega). \quad (2-15)$$

Figure 2-3 shows an application of the combined low pass and high pass Butterworth filters to a Fourier spectrum, in which dotted red curve is the original Fourier spectrum while the solid blue curve is the filtered one. The cutoff frequencies used are 0.2 Hz and 10 Hz in this example.

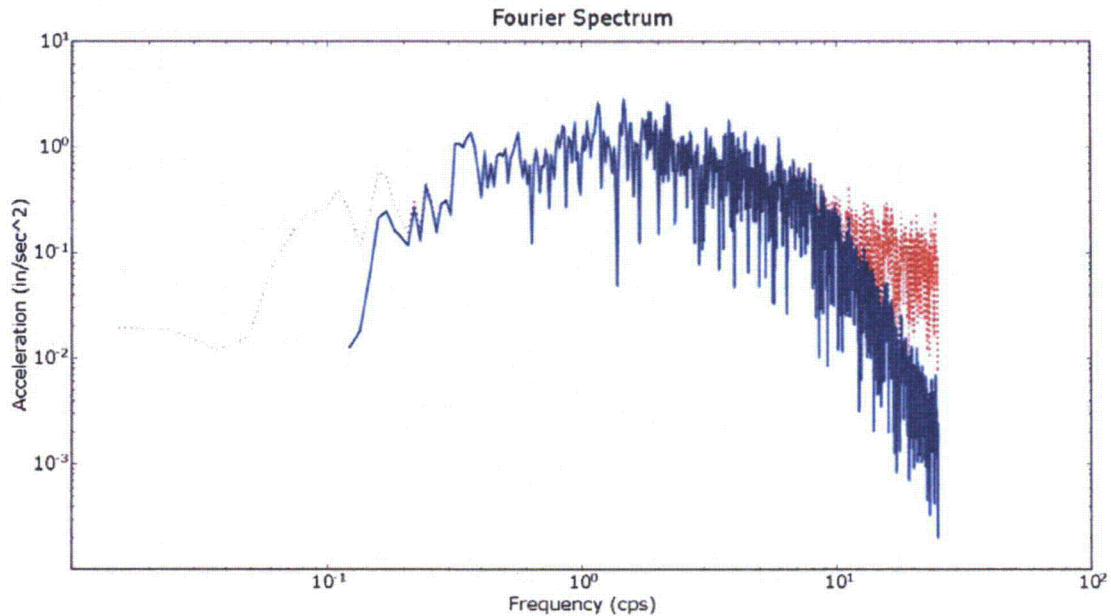


Figure 2-3 Application of Band Pass Butterworth Filter to A Fourier Spectrum

2.1.5 Fourier Components Smoothing

The triangular window smoothing method is implemented in P-CARES to smooth the Fourier components in order to eliminate the noises. It is very helpful in comparing two similar Fourier spectra, for example, one from a recorded record and the other from a computed record. The triangular window is defined by the width of the frequency window, i.e., the window frequency ω_w . In P-CARES, either a fixed-width frequency window or a varying-width frequency window can be specified by the user. The varying width frequency window, the width of which is defined by a percentage of the central frequency f_0 under consideration (e.g., $\omega_w = 20\% f_0$, see Appendix A to SRP 3.7.1, NUREG-0800), can lead to a constant width in the log scale. This smoothing method is basically a moving average algorithm with the weighting function shaped as a triangle, which is defined as,

$$w_i = \frac{N_{half} + i + 1}{(N_{half} + 1)^2}, \quad \text{for } i = -N_{half}, \dots, 0 \quad (2-16)$$

$$= w_{-i}, \quad \text{for } i = 1, \dots, N_{half}$$

where N_{half} is the integer half width of the frequency window, and is defined using the window frequency ω_w and the frequency increment δ_ω as,

$$N_{half} = \text{Floor}\left(\frac{\omega_w}{2\delta_\omega}\right) \quad (2-17)$$

in which Floor() is the mathematical function to truncate a real number to a integer. It should be noted that the sum of the weights of a full window is unity. The moving average algorithm can be described by the following updating equation,

$$F_i' = \sum_{j=-N_{half}}^{N_{half}} w_j F_{i+j} \quad (2-18)$$

Special considerations are given in the moving average algorithm when it approaches both ends of a Fourier spectrum where the number of frequencies left is fewer than the half window. For a fixed-width window approach, the few frequencies at the beginning are not smoothed and the few frequencies at the end are smoothed using a smaller window width. For the varying-width window approach, there is no such problem at the low frequency end, while smaller window is used for the high frequency end.

Figure 2-4 shows a Fourier spectrum being smoothed by a triangular window with the window frequency equal to 0.5 Hz, and Figure 2-5 shows the same Fourier spectrum being smoothed by a varying-width window with $\omega_w = 20\% f_0$. The varying-width window approach obviously yields a smoother curve in the high frequency range than the fixed-window approach.

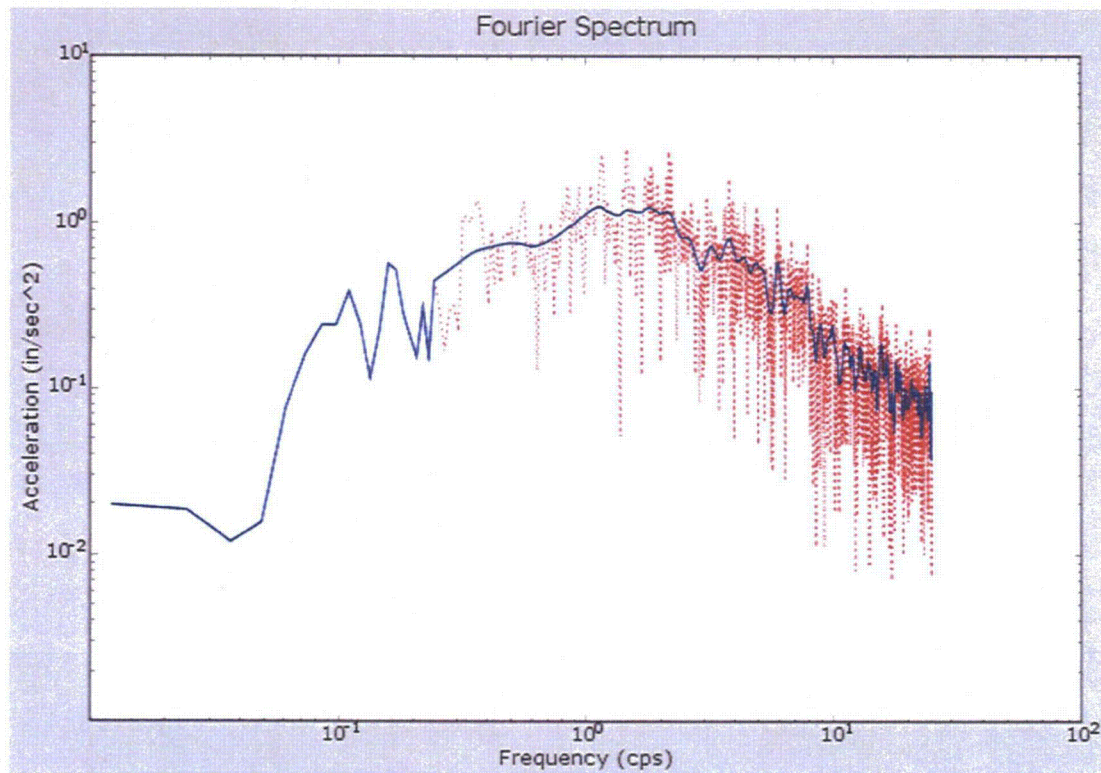


Figure 2-4 Application of Triangular Window Smoothing (Fixed-Width)

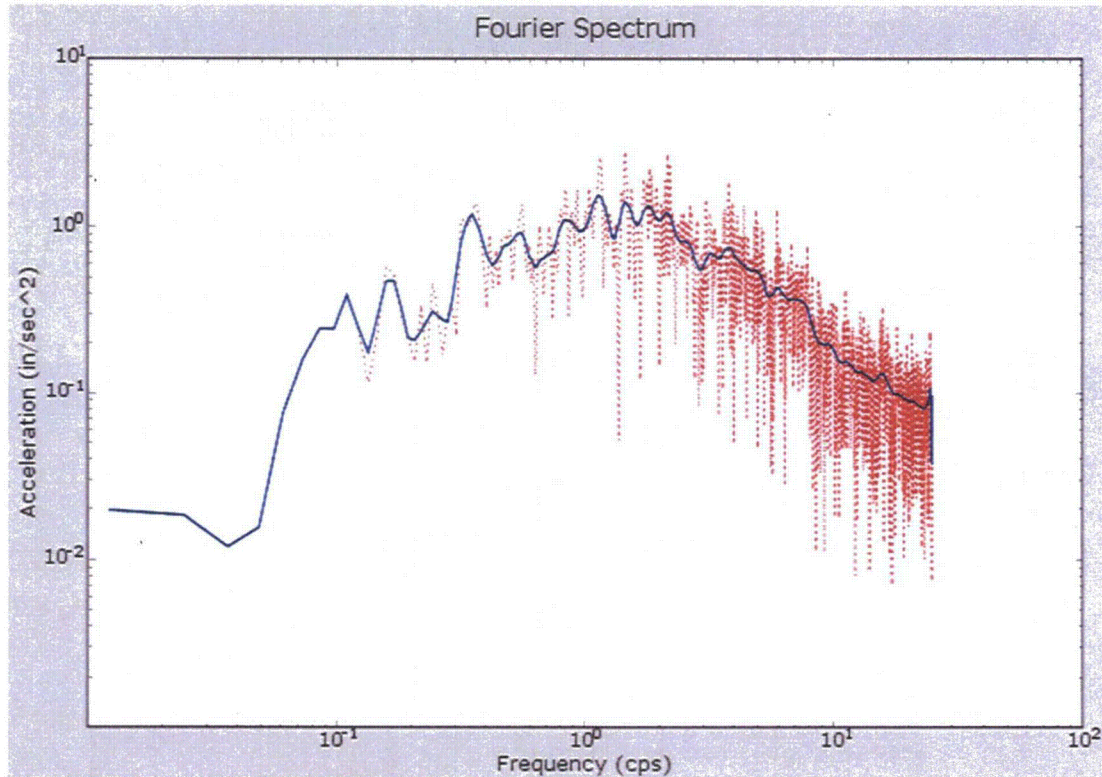


Figure 2-5 Application of Triangular Window Smoothing (Varying Width)

2.1.6 Response Spectrum

A response spectrum of a given motion is the maximum response of a linear oscillator of single degree of freedom, as a function of the fundamental frequency of the oscillator, where the given motion is the exciting motion to the oscillator. The governing equation of motion for the linear oscillator (see Figure 2-6) is,

$$z'' + 2\omega\zeta z' + \omega^2 z = -y'' \quad (2-19)$$

in which z is the relative motion between the mass and the base, y is the base motion, and ω and ζ are the fundamental and damping of the oscillator (Xu et al, 1990). Solution of Equation 2-19 must be obtained for each of the interested frequencies and damping values; the maximum of the acceleration experienced by the oscillator is commonly plotted with respect to the frequency as the response spectrum. The response spectra plot is often parameterized for multiple damping values.

Suppose the motion is an accelerogram with the time increment δt and a maximum duration T , P-CARES limits the maximum frequency on its response spectra with the Nyquist frequency,

$$f_{\max} = 1/2\delta t \quad (2-20)$$

The minimum spectra frequency is set equal to 0.1 Hz.

The algorithm in P-CARES to generate a response spectrum from an accelerogram utilizes a closed form solution of Equation 2-19 rather than a numerical integration method (e.g. Wilson's θ method). Assuming linear relation between two consecutive acceleration data points, Equation 2-19 between the two time stations t_j and t_{j+1} can be solved analytically (Nigam and Jennings

1968, Xu et al, 1990). Given the acceleration, velocity, and the displacement of the oscillator at t_j , the acceleration, velocity, and displacement at t_{j+1} can be analytically determined. Starting with a rest condition at time 0, the absolute acceleration of the oscillator at all time stations can be calculated in sequel, and the maximum value of these acceleration values becomes the spectral value at the particular frequency and damping.

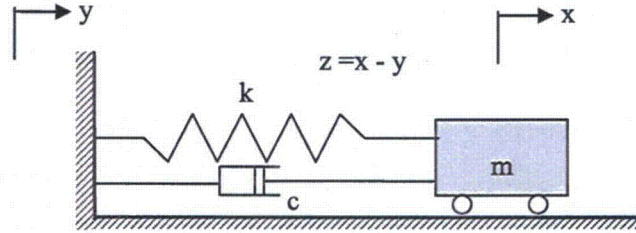


Figure 2-6 Illustration of a Linear Oscillator

2.1.7 Power Spectral Density and Coherency

Power Spectral Density (PSD) describes the distribution of power in an acceleration record with respect to frequency. Beyond this general and simplistic description, PSD has several different definitions in the literature (e.g., ASCE43-05, Bendat and Piersol, 1986, Proakis and Manolakis, 1988, and Press et al, 1990), depending on the purposes of the application. The one implemented in P-CARES follows the definition by Bendat and Piersol (1986) for compatibility with the coherency measures to be introduced later. For an acceleration function $x(t)$ of duration T , which is considered in terms of random process as a realization from its associated sample space Ω_a , its Fourier transform $X(f)$ and its one-sided power spectral density function $\Phi(f)$ can be defined as,

$$X(f, T) = \frac{1}{T} \int_0^T x(t) e^{-i2\pi ft} dt \quad (2-21)$$

$$\Phi_{XX}(f) = 2 \lim_{T \rightarrow \infty} \frac{1}{T} E[|X(f, T)|^2], \quad (2-22)$$

where the expectation $E[\]$ operates over the sample space Ω_a , and the limiting operation $T \rightarrow \infty$ cannot be performed in practice because the duration T can never be infinite. Note that the expectation operator in Equation 2-22 is required to ensure the resulting PSD function pairs with the corresponding correlation function by the Fourier transform. For a stationary process, the expectation can be estimated by averaging several records of duration T , and the power spectral density defined by Equation 2-22 gains its discrete format,

$$\hat{\Phi}_{XX}(f_k) = \frac{1}{N_{\Omega_a}} \sum_{i=1}^{N_{\Omega_a}} \frac{2}{T} |\hat{X}(f_k, T)|^2, \quad (2-23)$$

where N_{Ω_a} is the number of records used in the estimation, and the hat embellishment signifies the discrete version, and k indicates the k^{th} frequency in the spectra. However, in the context of seismic motions that are nonstationary processes, the expectation cannot be carried out using Equation 2-23, and the power spectral density must be approximated either by simply dropping the averaging operation or by locally averaging over a window in a single series of Fourier

components. The locally averaging technique, often named as window smoothing, is most commonly used in the coherency study.

Similarly, the one-sided cross spectral density for given Fourier spectra X and Y and its corresponding discrete version without taking the expectation are given by,

$$\Phi_{XY}(f) = 2 \lim_{T \rightarrow \infty} \frac{1}{T} E[X^*(f, T)Y(f, T)] \quad (2-24)$$

$$\hat{\Phi}_{XY}(f_k) = \frac{2}{T} \hat{X}^*(f_k, T)\hat{Y}(f_k, T), \quad (2-25)$$

where X^* is the complex conjugate of X .

For two seismic motions recorded at two locations, the coherency between them, a dimensionless measure, is defined by the smoothed cross power spectrum that is normalized by the corresponding auto power spectra of these two motions (Abrahamson, 2006, Zerva and Zervas, 2002), i.e.,

$$\gamma_{XY}(\omega) = \frac{\Phi_{XY}(\omega)}{\sqrt{\Phi_{XX}(\omega)\Phi_{YY}(\omega)}}. \quad (2-26)$$

The coherency $\gamma_{XY}(\omega)$ is a complex number and can be shown with a magnitude within the range [0, 1]. If the spectra used in the above definition are not locally smoothed, the magnitude of $\gamma_{XY}(\omega)$ is unity for all frequencies. The absolute value (magnitude) of coherency, $|\gamma_{XY}(\omega)|$, is designated as the lagged coherency, which measures the phase variation between the two motions. The phase spectrum is defined by the phase angle in $\gamma_{XY}(\omega)$ as $\tan^{-1}(\text{real}(\gamma_{XY}(\omega))/\text{imag}(\gamma_{XY}(\omega)))$. The unlagged coherency is defined as the real($\gamma_{XY}(\omega)$). $\text{Tanh}^{-1}(|\gamma_{XY}(\omega)|)$ is approximately normally distributed, and is termed in P-CARES as ‘‘Arctanh Coherency’’.

In the context of computing the coherency measures, the accelerograms are first tapered by a split cosine bell taper function to reduce the power leakage effect. This taper function is defined as,

$$x(t) = \begin{cases} 0.5(1 - \cos(2\pi / pT)), & \text{if } t \leq 0.5pT \\ 1.0, & \text{if } 0.5pT < t \leq (1-0.5p)T \\ 0.5(1 - \cos(2\pi(T-t) / pT)), & \text{if } (1-0.5p)T < t \end{cases} \quad (2-27)$$

where p is the percentage of the duration T that will be tapered at both ends. The Hamming’s window, with the number of point being specified by the user, is applied to locally smooth the cross and auto power spectra used in the various coherency measures. The Hamming’s window is given by,

$$w(k) = 0.53836 + 0.46164 \cos(k\pi / M), \quad k = -M, \dots, -1, 0, +1, \dots, M \quad (2-28)$$

where $2M+1$ is the window width (the number of frequencies used in the smoothing).

2.1.8 Time History Synthesis

In light of Equation 2-1, an acceleration record can be generated by properly computing the array of Fourier coefficients A_j such that the generated time history has the desired characteristics of observed seismic motions. Given a target response spectrum, a synthetic time history matching this response spectrum is generated by the following iterative procedure in P-CARES.

The amplitudes of the Fourier components A_j (see Equation 2-1) are first initiated with the values determined from the input target response spectrum. The corresponding phase angles are then generated as an array of random values uniformly distributed in the range $[0, 2\pi]$. From these trial Fourier components ($|A_j|$ and their phase angles), a trial acceleration time history is generated using the inverse FFT algorithm. The acceleration record is then undergone three enhancing modifications that are to be introduced later in this subsection. The Fourier components A_j are updated accordingly by the FFT algorithm using the modified acceleration record, and a trial response spectrum of this record is calculated as well. By comparing this trial response spectrum to the desired target response spectrum, the Fourier components are modified by the following relation,

$$A_j^{new} = A_j^{old} \frac{R_{target}}{R_{trial}} \quad (2-29)$$

where the terms R refer to the values of the response spectra at the frequency ω_j , and the calculation is in complex domain. The phase angles originally generated at the first trial are maintained by the above updating relation (Equation 2-29) and will not be regenerated in later iterations. The new Fourier components are then used to form a new trial acceleration time history and the process is repeated. If the process does not reach a satisfactory convergence after a number of trials, the whole process should be restarted with an array of newly generated phase angles that will generally be different from the first set.

During each iteration cycle, three modifications to the trial acceleration record are involved to improve the generated accelerogram so that it resembles the characteristics of realistic earthquake records. The first of these modifications is to incorporate the nonstationarity characteristic observed in measured earthquake records into the generated record. This is accomplished in P-CARES by multiplying a deterministic enveloping function $E(t)$ on the generated sinusoidal motions (Equation 2-1), i.e.,

$$a(t) = E(t) \sum_{j=0}^{m-1} A_j e^{i\omega_j t} \quad (2-30)$$

where the coefficients A_j are complex. The enveloping function $E(t)$ that has been selected in P-CARES is a simple trilinear function consisting of a parabolic rise to unity at a rise time T_r , a plateau of value unity for the strong motion duration T_s , and an exponential ramp down to zero for a decay time T_d . The total duration of the enveloping function T_E is then the sum of the rise time, the strong motion duration, and the decay time, which are functions of the earthquake magnitude M , or

$$T_E(M) = T_r(M) + T_s(M) + T_d(M) \quad (2-31)$$

These time parameters as functions relating to a specified earthquake magnitude estimate (M) are determined by fitting empirical data obtained from Salmon et al (1992). The purpose of this approach is to arrive at reasonable (or realistic) estimates of the synthetic accelerograms for use in response studies. Given an estimate of the earthquake magnitude (usually the magnitude scale M_w , defined based on the seismic moment), P-CARES can calculate the controlling parameters of the enveloping function. In the P-CARES implementation, these calculated duration values can be changed by user input and therefore only serve as guidelines. The total duration of the motion is taken as the larger of $T_E(M)$ from Equation 2-31 and the desired maximum duration input T_{max} . If $T_E(M)$ is less than the desired duration T from Equation 2-4, the generated acceleration record is padded with zeros from $T_E(M)$ to T . Please note that recent works using more extensive recorded data may suggest better parameters for Equation 2-31 (e.g., McGuire et al, 2001), but may require a sizeable effort to abstract them out of the data.

The second modification included in the motion generation algorithm is a baseline correction algorithm to make the ground velocity and displacement reach zero at the end of the motion. The Lagrange multiplier based utility described in Section 2.1.2 is directly used for this purpose. The generated accelerogram is baseline corrected during each trial iteration. The influence of the correction is small in terms of accelerations (high frequency content) but may be significant in the lower frequency range where velocity and displacement characteristics become important.

The last modification incorporated in the motion algorithm, termed "cutting and flipping", is to ensure the target peak acceleration is not exceeded by the generated acceleration record. If any acceleration value in the trial record exceeds the target peak acceleration, it is flipped around the target peak acceleration, i.e. by subtracting the twice of the difference between this acceleration value and the target peak. The purpose of this approach is (a) to limit the peak accelerations to the desired target and (b) to allow the generated record maintain a realistic (randomized) shape, instead of generating flat spots by simply cutting the peaks of the record.

2.2 Free-Field Analysis

As a simple and often adequate approximation, free-field analysis herein considers only the vertical propagation of horizontal earthquake ground motions based on the assumption that one dimensional horizontal shear wave propagates vertically from the bedrock through the soil deposit to the ground surface. This type of analysis is typically performed by using either a discrete method based on finite element procedures (e.g. the FLUSH Code approach) or by using a continuous method based on the solution to the one dimensional wave equation (e.g., the SHAKE Code approach). The objective of this analysis is to determine the horizontal motion-time histories (accelerograms) developed at any depth of a horizontally stratified soil system, when a specified accelerogram is input at any of the soil layer interfaces or at the rock outcrop.

The method employed in the P-CARES for free-field analysis is the continuous solution model. A given soil column is assumed to be composed of a number of uniform soil layers of arbitrary thickness; each layer is assumed to be linear elastic with soil properties that are constant throughout its thickness. Such a typical configuration involving N layers is shown in Figure 2-7.

Vertical shear wave propagation through this layered system produces horizontal stresses and accelerations which satisfy the shear wave equation for each soil layer. The stress-strain relation for each layer is specified in the form:

$$\tau = G\gamma + \eta\dot{\gamma} \quad (2-32)$$

where τ , γ , G , and η are the shear stress, the shear strain, the shear modulus, and the viscosity coefficient of a given soil layer respectively. The term $\dot{\gamma}$ is the differentiation of the shear strain with respect to time. The shear wave equation for each layer is:

$$\rho \frac{\partial^2 u}{\partial t^2} = G \frac{\partial^2 u}{\partial x^2} + \eta \frac{\partial}{\partial t} \left[\frac{\partial^2 u}{\partial x^2} \right] \quad (2-33)$$

where u is the total horizontal displacement of any point in the layer, t represents time, ρ is the mass density of the soil layer, and x is the coordinate of a point in the soil column, which originates at the ground surface and is positive downward (see Figure 2-7).

As assumed above, each soil material in the column is treated as linear elastic, including both shear stiffness and damping properties. This linear relation has often been used for seismic applications (e. g., Seed and Idriss, 1970), provided that the damping parameter η is interpreted as representing a mechanism to dissipate energy per strain cycle as found from tests for the actual

nonlinear behavior of the soil under cyclic shear loadings, as for example in the resonant column shear test. The energy lost per loading cycle due to the actual nonlinear behavior is measured by the hysteretic damping ratio, D , which has been found experimentally to be reasonably independent of frequency, particularly in the low frequency ranges of interest to structural response. If this energy loss per cycle is equated to the energy loss per cycle due to the linear viscosity term in Equation 2-32, the hysteretic damping ratio D is found to be related to the viscosity coefficient η by,

$$D = \frac{\eta\omega}{2G} \quad (2-34)$$

where ω is the circular frequency of the motion component and G is the soil shear modulus.

Considering steady-state motions at a given forcing frequency ω and applying the Fourier transform to Equation 2-33, the equation of motion becomes,

$$(G + i\omega\eta) \frac{\partial^2 U}{\partial x^2} + \rho\omega^2 U = 0 \quad (2-35)$$

where U is the Fourier transform of the horizontal displacement u at an arbitrary depth x . Using the hysteretic damping ratio D , the complex shear modulus of the material in the above equation becomes,

$$G^* = G(1 + i2D) \quad (2-36)$$

and Equation 2-35 can be simplified to :

$$\frac{\partial^2 U}{\partial x^2} + (k^*)^2 U = 0 \quad (2-37)$$

where the complex wave number k^* is defined as,

$$(k^*)^2 = \frac{\rho\omega^2}{G^*} \quad (2-38)$$

Solving Equation 2-37 yields:

$$U_j = A_j \exp(+ik_j^*x) + B_j \exp(-ik_j^*x) \quad (2-39)$$

where A_j and B_j represent the magnitudes of the incident and reflected waves respectively, at the interface j (at the bottom of layer j). The boundary and interface conditions at the ground surface and between soil layers are

$$\begin{aligned} T_1(x=0) &= 0 \\ U_j(x=x_j) &= U_{j+1}(x=x_j) \\ T_j(x=x_j) &= T_{j+1}(x=x_j) \end{aligned} \quad (2-40)$$

in which T is the Fourier transform of the shear stress τ . Applying the conditions of Equations 2-40 to Equations 2-39, the coefficients A_{j+1} and B_{j+1} at a given layer interface $j+1$ are determined in terms of the coefficients A_j and B_j at the previous layer j by:

$$\begin{aligned} A_{j+1} &= \frac{1}{2} \left\{ A_j \left(1 + \frac{k_j^* G_j^*}{k_{j+1}^* G_{j+1}^*} \right) \exp[ix_j(k_j^* - k_{j+1}^*)] + B_j \left(1 - \frac{k_j^* G_j^*}{k_{j+1}^* G_{j+1}^*} \right) \exp[-ix_j(k_j^* + k_{j+1}^*)] \right\} \\ B_{j+1} &= \frac{1}{2} \left\{ A_j \left(1 - \frac{k_j^* G_j^*}{k_{j+1}^* G_{j+1}^*} \right) \exp[ix_j(k_j^* + k_{j+1}^*)] + B_j \left(1 + \frac{k_j^* G_j^*}{k_{j+1}^* G_{j+1}^*} \right) \exp[-ix_j(k_j^* - k_{j+1}^*)] \right\} \end{aligned} \quad (2-41)$$

Calculations begin by assuming the coefficient A_0 at the top of the first layer (ground surface) to be unity (i.e, the real and imaginary components are 1,0). Applying the known shear stress condition at the ground surface yields the coefficient B_1 equal to A_1 . All the remaining coefficients can then be solved recursively from Equation 2-41. At the layer interface where the input ground motion is specified, the acceleration magnitude from the calculation is compared with the known acceleration magnitude, and a correction factor is determined as the ratio of the known acceleration magnitude to the calculated acceleration magnitude. The coefficients A_i 's and B_i 's, calculated above by assuming $A_0 = B_0 = 1$, are then corrected by multiplying this correction factor. If an outcrop is defined at the bottom of the soil column, the motion at the outcrop is determined by considering that the shear stress at the outcrop is equal to zero and the incident wave from the soil column solution is the same as the incident wave for the uniform half-space. Because of the zero stress condition at the outcrop, the reflected wave solution can be written in terms of the incident wave solution of the half-space.

P-CARES requires that the soil properties for each soil layer, low strain shear modulus (G_{max}), the soil unit weight (γ), and the thickness (H), be specified including their probability distribution. Half-space properties are also required if the half-space is to be considered in the analysis. The nonlinear behavior of the actual soil is considered in the linear analysis in P-CARES by employing strain-compatible soil degradation models for soil modulus and damping properties, as listed below:

- a. Seed-Idriss 1970 (Seed and Idriss, 1970),
- b. Idriss 1990 (Idriss, 1990),
- c. GEI Original From SRS (GEI, 1983),
- d. Stokoe SRS 1995 (Stokoe et al, 1995),
- e. Geomatrix 1990 (Coppersmith, 1991),
- f. EPRI-93 Cohesionless Soil (EPRI, 1993),
- g. constant damping and no reduction in the shear modulus, or
- h. a user specified degradation model.

The specific degradation curves for the first six models contained in P-CARES are listed in Table 2-1.

An iterative procedure similar to that of SHAKE (Schabel et al, 1972) is used to account for nonlinear soil behavior within the context of this linear analysis. Calculations are performed by initially assuming an initial trial value of effective shear strain within each soil layer. Given the effective shear strain, the shear modulus and hysteretic damping for each soil layer are then determined on the soil degradation curves specified for each layer. At the end of each computational cycle, the calculated effective shear strain is computed and compared with the assumed trial value. When the assumed and calculated shear strains differ by less than 5% for all soil layers, the solution is considered to have converged. The strains are computed at the top and bottom of each soil layer and averaged to determine the effective strain for the layer.

Two approaches can be chosen in P-CARES to calculate the maximum effective strain. In the first approach, the maximum strain is computed in the time domain for each soil layer. The Fourier components of shear strain are combined using the inverse FFT algorithm to obtain the actual maximum shear strain developed in each soil layer during the course of the motion. The effective cyclic shear strain developed in the layer is then estimated from the maximum strain by

$$\gamma_{effective} = 0.65\gamma_{max} \quad (2-42)$$

This effective cyclic shear strain is then used to obtain the effective shear modulus and damping ratio on the specified soil degradation curves; the new effective shear modulus and damping ratio are used for response computation in the next iteration.

In an alternative approach available in P-CARES to approximate the effective cyclic shear strain, the maximum shear strain can be estimated from the RMS strain values, eliminating the need for conversion to the time domain from the frequency domain. The relationship used for this estimation is

$$\gamma_{\max} = \gamma_{RMS} \left[\frac{a_{\max}}{a_{RMS}} \right] \quad (2-43)$$

where the term in parenthesis is the ratio of the peak to the RMS value of the input acceleration record. The effective strain is then calculated from Equation 2-42 above. It should be noted that although the maximum strain calculated directly in the time domain is more accurate, it is a slower calculation and has been found to not differ significantly from the RMS strain calculated in the frequency domain.

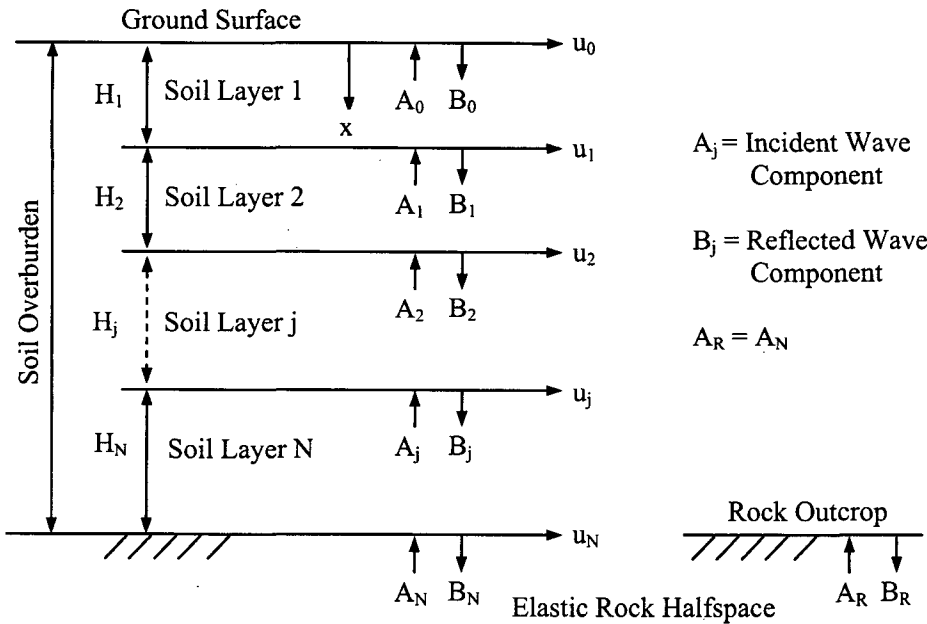


Figure 2-7 Soil Column and Rock Outcrop Motion

Table 2-1 Soil Degradation Models
Shear Modulus Ratio - G/Gmax

SHEAR STRAIN (%)	SEED-IDRISS 70		IDRISS 1990		GEI Original From SRS				
	SAND	CLAY	SAND	CLAY	0'-50'	50'-100'	100'-250'	250'-500'	500'+
0.000100	1.000	1.000	1.000	1.000	1.000	1.000	1.000	1.000	1.000
0.000316	0.984	0.913	1.000	1.000	0.990	0.990	0.990	0.995	1.000
0.00100	0.934	0.761	0.990	1.000	0.980	0.980	0.980	0.990	1.000
0.00316	0.826	0.565	0.955	0.979	0.910	0.935	0.947	0.965	0.985
0.0100	0.656	0.400	0.850	0.941	0.780	0.816	0.852	0.890	0.925
0.0316	0.443	0.261	0.628	0.839	0.560	0.610	0.670	0.725	0.775
0.100	0.246	0.152	0.370	0.656	0.330	0.360	0.425	0.495	0.565
0.316	0.115	0.076	0.176	0.429	0.160	0.175	0.200	0.240	0.300
1.00	0.049	0.037	0.080	0.238	0.065	0.065	0.065	0.080	0.100
3.16	0.049	0.013	0.080	0.238	0.040	0.040	0.040	0.040	0.040
10.00	0.049	0.004	0.080	0.238	0.040	0.040	0.040	0.040	0.040

Shear Modulus Ratio - G/Gmax (Continued)

SHEAR STRAIN (%)	STOKOE SRS 1995					
	UPLAND SAND	TOBACCO ROAD	DRY BRACH	SHALLOW CLAYS	DEEP SANDS	DEEP CLAYS
0.000100	0.9953	0.9977	0.9987	0.9993	0.9991	0.9996
0.000316	0.9852	0.9929	0.9959	0.9979	0.9972	0.9986
0.00100	0.9545	0.9778	0.9872	0.9933	0.9911	0.9957
0.00316	0.8691	0.9329	0.9606	0.9791	0.9723	0.9864
0.0100	0.6774	0.8148	0.8851	0.9367	0.9174	0.9583
0.0316	0.3991	0.5818	0.7089	0.8239	0.7783	0.8791
0.100	0.1736	0.3056	0.4350	0.5968	0.5261	0.6970
0.316	0.0623	0.1221	0.1958	0.3188	0.2598	0.4211
1.00	0.0206	0.0421	0.0715	0.1289	0.0999	0.1870
3.16	0.0066	0.0137	0.0238	0.0447	0.0339	0.0678
10.00	0.0021	0.0044	0.0076	0.0146	0.0110	0.0225

Shear Modulus Ratio - G/Gmax (Continued)

SHEAR STRAIN (%)	GEOMATRIX 1990			EPRI-93 COHENSIONLESS SOIL					
	0'-50'	50'-150'	150'+	0'-20'	20'-50'	50'-120'	120'-250'	250'-500'	500'-1000'
0.000100	1.000	1.000	1.000	1.000	1.000	1.000	1.000	1.000	1.000
0.000316	0.991	0.999	1.000	1.000	1.000	1.000	1.000	1.000	1.000
0.00100	0.985	0.998	1.000	0.979	0.992	0.995	0.998	1.000	1.000
0.00316	0.943	0.975	0.999	0.903	0.940	0.951	0.972	0.980	0.992
0.0100	0.854	0.900	0.939	0.734	0.815	0.867	0.899	0.923	0.948
0.0316	0.688	0.767	0.826	0.488	0.589	0.665	0.726	0.774	0.834
0.100	0.454	0.536	0.620	0.266	0.355	0.427	0.492	0.557	0.645
0.316	0.259	0.319	0.381	0.113	0.161	0.210	0.266	0.315	0.395
1.00	0.100	0.134	0.162	0.044	0.065	0.089	0.117	0.153	0.202
3.16	0.052	0.052	0.052	0.044	0.065	0.089	0.117	0.153	0.202
10.00	0.052	0.052	0.052	0.044	0.065	0.089	0.117	0.153	0.202

Hysteretic Damping Ratio (%)

SHEAR STRAIN (%)	SEED-IDRISS 70		IDRISS 1990		GEI Original From SRS				
	SAND	CLAY	SAND	CLAY	0'-50'	50'-100'	100'-250'	250'-500'	500'+
0.000100	0.50	2.50	0.24	0.24	1.50	1.50	1.50	1.50	1.50
0.000316	0.80	2.50	0.44	0.44	1.50	1.50	1.50	1.50	1.50
0.00100	1.70	2.50	0.80	0.80	1.50	1.50	1.50	1.50	1.50
0.00316	3.20	3.50	1.46	1.46	1.75	1.60	1.50	1.50	1.50
0.0100	5.60	4.75	2.80	2.80	3.85	3.15	2.50	2.10	1.75
0.0316	10.00	6.50	5.31	5.31	7.75	6.50	5.00	3.75	2.50
0.100	15.50	9.25	9.80	9.80	13.10	11.75	10.00	8.25	6.25
0.316	21.00	13.80	15.74	15.74	18.75	17.75	16.50	14.75	13.00
1.00	24.60	20.00	21.00	21.00	23.00	22.50	22.00	20.50	19.00
3.16	24.60	26.00	21.00	21.00	26.00	25.60	25.40	24.25	23.10
10.00	24.60	29.00	21.00	21.00	26.00	25.60	25.40	24.25	23.10

Hysteretic Damping Ratio (%) (Continued)

SHEAR STRAIN (%)	STOKOE SRS 1995					
	UPLAND SAND	TOBACCO ROAD	DRY BRACH	SHALLOW CLAYS	DEEP SANDS	DEEP CLAYS
0.000100	1.059	0.625	0.825	1.296	0.489	0.991
0.000316	1.151	0.670	0.846	1.296	0.505	0.991
0.00100	1.493	0.835	0.936	1.326	0.57	1.013
0.00316	2.434	1.300	1.205	1.456	0.759	1.097
0.0100	5.201	2.790	2.108	1.938	1.398	1.41
0.0316	10.407	6.139	4.336	3.233	3.039	2.276
0.100	15.000	12.799	9.605	6.82	7.289	4.856
0.316	15.000	15.000	15.000	12.884	13.799	9.833
1.00	15.000	15.000	15.000	15.000	15.000	12.995
3.16	15.000	15.000	15.000	15.000	15.000	12.995
10.00	15.000	15.000	15.000	15.000	15.000	12.995

Hysteretic Damping Ratio (%) (Continued)

SHEAR STRAIN (%)	GEOMATRIX 1990				EPRI-93 COHENSIONLESS SOIL					
	0'-50'	50'-150'	150'-300'	300'+	0'-20'	20'-50'	50'-120'	120'-250'	250'-500'	500'-1000'
0.000100	0.21	0.15	0.15	0.96	1.43	1.30	1.15	0.95	0.85	0.61
0.000316	0.21	0.15	0.15	0.98	1.43	1.30	1.15	0.95	0.85	0.61
0.00100	2.05	1.52	1.52	1.01	1.84	1.43	1.22	1.02	0.90	0.61
0.00316	2.50	1.95	1.68	1.01	2.76	2.04	1.63	1.33	1.02	0.71
0.0100	3.73	2.95	2.25	1.07	5.10	3.67	2.86	2.24	1.84	1.22
0.0316	6.56	4.73	3.22	1.56	9.39	7.14	5.51	4.49	3.57	2.55
0.100	11.23	8.57	6.19	4.15	15.51	12.55	10.41	8.67	7.14	5.31
0.316	15.98	13.07	10.27	7.84	22.25	19.39	17.04	15.10	13.27	10.61
1.00	21.09	18.59	15.66	12.08	27.55	24.90	22.86	21.12	19.39	16.73
3.16	24.11	24.11	24.11	17.84	27.55	24.90	22.86	21.12	19.39	16.73
10.00	24.11	24.11	24.11	17.84	27.55	24.90	22.86	21.12	19.39	16.73

2.3 Kinematic Interaction Algorithm

The presence of the foundation of a structure in the soil system changes the free-field motion because of the kinematic interaction effect. The kinematic interaction refers to the case that the free-field motion is modified when assuming the foundation be massless and rigid. This section of the report discusses the methods used in P-CARES to treat the kinematic interaction effect. It should be noted that kinematic effects do not exist for surface foundations and are small for those problems where the maximum frequency of interest f^* is less than:

$$f^* = V_s / 2\pi R \quad (2-44)$$

where V_s is the shear wave velocity and R is the foundation radius.

This module in P-CARES begins with free-field accelerograms defined over the depth of the foundation (determined in the free-field analysis module) and generates equivalent translational and rotational motions of the foundation to be used as input to the structural analysis module. The general formulation of the methods used to treat these effects is discussed first, and is followed with a description of the procedure used to incorporate the effects into the P-CARES system.

2.3.1 General Formulation

The method proposed by Iguchi (1982) and further discussed by Pais and Kausel (1985) is used to incorporate the kinematic interaction effect in P-CARES. The method is illustrated in Figure 2-8 (see Fig. 39 of Pais and Kausel, 1985) and consists of the following steps:

1. Evaluate the free-field motion and stresses at several depths covering the foundation depth. The free-field motion is obtained from the free-field analysis module and the evaluation of the stresses is discussed below in Section 2.3.2.
2. Obtain a best-fit rigid body deformation (basemat displacement and rotation) of the foundation to the free-field motion.
3. Determine forces acting on the foundation by integrating the free-field stresses over the surface of the foundation.
4. The forces found in step (3) must be eliminated because the foundation is assumed massless in the kinematic interaction analysis. Deformations required to eliminate these forces are determined using the soil-structure interaction coefficients.
5. The input motion to the structure is then the sum of the deformations determined in steps (2) and (4). These deformations consist of displacement and rotation at the basemat and are used as input to the structural analysis module.

These five steps are performed in the frequency domain, and will be discussed in detail in the following subsections.

2.3.2 Free-field Solution and Shear Stress Evaluation

The free-field accelerations are determined in the free-field analysis module based on a model of vertically propagating, horizontally polarized shear waves. P-CARES integrates the kinematic interaction analysis module into the free-field analysis module to streamline the soil-structure interaction process. By specifying a few parameters needed in the kinematic interaction analysis, P-CARES can automatically generate the required free-field motions over the whole depth of

foundation and calculate the translational and rotational displacements at the basemat. The variation of free-field motion with depth z is a function of $\cos(\omega z/V_s)$, where V_s is the shear wave velocity. The number of output motions required to cover the foundation depth should be sufficiently large so that at least three points are contained within a half cosine wave, i.e., the difference between two nearby output depths should be

$$dz = \pi V_s / 6\omega = V_s / 12f \quad (2-45)$$

where f is the maximum frequency of interest in the problem. P-CARES allows the user to select the maximum frequency of interest, calculates dz using above equation, and then generates free-field solutions at depths equally spaced over the foundation depths at an increment not exceeding dz . Depths at the ground surface and the basemat are included in the output depths generated by P-CARES.

The free-field stresses are then evaluated within kinematic interaction module based on the specified displacements. The displacements u_{ij} at depth z_i and frequency ω_j are defined as:

$$u_{ij} = a_{ij} \cos \omega_j t + b_{ij} \sin \omega_j t \quad (2-46)$$

where a_{ij} and b_{ij} are the Fourier Components of the output motion at depth z_i . The displacement at an arbitrary depth z and a given frequency ω_j can be represented as a polynomial of order $N-1$ in z , where N is the number of depths used to define the free-field displacements so that:

$$u(z, \omega_j) = (c_1 + c_2 z + \dots + c_N z^{N-1}) \cos(\omega_j t) + (s_1 + s_2 z + \dots + s_N z^{N-1}) \sin(\omega_j t) \quad (2-47)$$

The coefficients c 's and s 's can be determined by solving the system of equations that are obtained by equating the previous two definitions of u (Equations 2-46 and 2-47)

The shear stresses are then found from:

$$\tau = G \frac{du}{dz} = G[(c_2 + \dots + c_N z^{N-2}) \cos(\omega_j t) + (s_2 + \dots + s_N z^{N-2}) \sin(\omega_j t)] \quad (2-48)$$

where, G is the soil shear modulus. This formula is then used to evaluate the shear stress at each layer and at each frequency. These operations to evaluate the shear stresses are contained within P-CARES and require no action by the user.

2.3.3 Best Fit

The next step in the solution is to obtain a rigid-body displacement of the foundation that is a best fit (in a least squared error sense) to the free-field motion. The motion of the rigid foundation can be conveniently represented by a horizontal displacement Δ_2 at the center of gravity of the foundation area and the rotation of the foundation Φ_2 about the centroidal axis. The subscript 2 indicates the displacements are the solution to the second step listed above in subsection 2.3.1. These two displacements are complex so that there are four components to be determined.

The best fit displacements for the cylindrical foundation are found to be:

$$\begin{aligned}\Delta_2 &= \left[\int_0^H 2\pi u(z)R dz + \pi R^2 u(H) \right] / A_c \\ \Phi_2 &= - \left[\int_0^H 2\pi u(z)(z - z_o)R dz + \pi R^2 u(H)(H - z_o) \right] / I_c\end{aligned}\quad (2-49)$$

where,

$u(z)$ = free - field motion at depth z

A_c = surface area of foundation = $\pi R^2 (1 + 2H / R)$

R = foundation radius

z_o = depth of the center of gravity below the surface = $H - R(H / R)^2 / (1 + 2H / R)$

H = depth of embedment

I_c = moment of inertia of foundation surface area about center of gravity

$$= \pi R^4 [1 + 4H / R + 8(H / R)^3 / 3 - 4(H / R)^4 / (1 + 2H / R)]$$

The integrals over the depth of the foundation H are evaluated by numerical integration in P-CARES.

The best fit displacements for the rectangular foundation, with plan dimensions $2B$ by $2L$, the deformations in the B direction, and embedment depth H , are found to be:

$$\begin{aligned}\Delta_2 &= [4B \int_0^H u(z) dz + 4u(H)BL] / A_r \\ \Phi_2 &= -[4B \int_0^H u(z)(z - H + z_o) dz + 4(H - z_o)u(H)BL] / I_r\end{aligned}\quad (2-50)$$

where,

A_r = surface area of foundation = $4H(B + L) + BL$

z_o = depth of center of gravity below the surface = $[2H^2(B + L) + BLH] / A_r$

I_r = moment of inertia of foundation surface area about center of gravity

$$= [4B^4 / 3] [(H / B)^3 (L / B + 1) + (H / B)(3L / B + 1) + L / B]$$

2.3.4 Determine Forces Acting on Foundation Area

The free-field stresses acting on the foundation area result in a horizontal force F and moment M , which can be obtained by integrating the free-field stresses over the foundation area. The resultant forces for the cylindrical foundation are:

$$\begin{aligned}F &= -\tau(H)\pi R^2 \\ M &= -4R^2 \int_0^H \tau(z) dz\end{aligned}\quad (2-51)$$

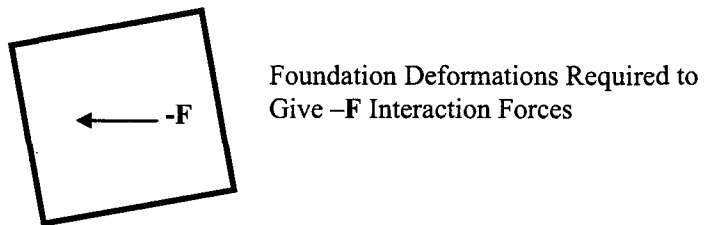
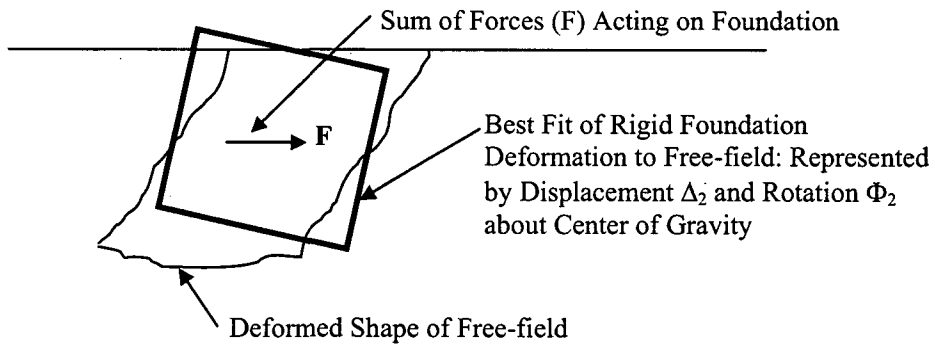
The resultant forces for the rectangular foundation are, assuming the motion is in the B direction:

$$\begin{aligned}F &= -4LB\tau(H) \\ M &= -4LB \int_0^H \tau(z) dz\end{aligned}\quad (2-52)$$

2.3.5 Eliminate Forces on Foundation

As indicated in step 4 in subsection 2.3.1, displacements Δ_4 and Φ_4 that eliminate the forces found in the previous subsection are found as follows. The stiffness and damping SSI coefficients are determined as discussed in the structural analysis module (see Section 2.4). These displacements can be determined by equating the forces to the matrix of SSI coefficients times the unknown displacements and solving the resultant system of equations for the unknown displacements.

The final displacements are taken as the sum of displacements Δ_4 and Φ_4 , and the displacements Δ_2 and Φ_2 found in Section 2.3.3. These final displacements are then translated to the base of the foundation from the center of gravity and saved for use as input to the structural analysis module.



Final Deformation of Foundation Is the Sum of the Above Two Solutions.

Figure 2-8 Illustration of Kinematic Interaction

2.4 Modeling of Structures and SSI

This section of the report describes the response analysis of a structural system subjected to either a seismic input at the base or time-dependent forcing functions applied to the structure. The solution method is first discussed, and followed is a description of each of the matrices used to represent the dynamic characteristics of the structure.

2.4.1 Description of the Model and Method of Solution

The structural model is based on the following basic assumptions:

- (a) All structural elements are linearly elastic.
- (b) The foundation of the structure may be assumed to be rigid (as compared to the surrounding soil and superstructure elements). This allows the use of existing soil / structure interaction (SSI) coefficients so that the soil does not need to be included in the structural model.
- (c) The soil properties may be modeled in two layers, one to the side of the structure and one beneath the structure. This is a necessary assumption since SSI coefficients are not generally available for more complex layering systems. The user may develop "equivalent" properties to approximately account for layering effects.
- (d) The length units must be in feet (the gravitational constant 32.2 ft/sec^2 is used within the code to convert weight to mass). Any consistent force units may be used.

The equations of motion representing the structural response are:

$$\mathbf{M}\mathbf{U}'' + \mathbf{C}\mathbf{U}' + \mathbf{K}\mathbf{U} = \mathbf{F}(t) \quad (2-53)$$

where \mathbf{M} , \mathbf{C} , \mathbf{K} , and \mathbf{F} represent the mass, damping, stiffness, and forcing matrices and are each discussed below. The deformation vector and its first and second derivatives with respect to time are \mathbf{U} , \mathbf{U}' , and \mathbf{U}'' . Bold variables are used in this discussion to represent matrices and vectors.

The deformation and force vectors can each be represented with their Fourier components as:

$$\begin{aligned} \mathbf{U}(t) &= S(\mathbf{U}_c \cos \omega t + \mathbf{U}_s \sin \omega t) \\ \mathbf{F}(t) &= S(\mathbf{F}_c \cos \omega t + \mathbf{F}_s \sin \omega t) \end{aligned} \quad (2-54)$$

where ω is the circular frequency and S is a scaling factor. The number of terms and frequency increment in these expansions are determined by the characteristics of the input forcing function \mathbf{F} .

The deformation vector U_i at each node i has 12 components that represent the combination of the 6 degrees of freedom and the two sine or cosine coefficients, i.e.,

$$\mathbf{U}_i = [ucx_i, usx_i, ucy_i, usy_i, ucz_i, usz_i, ucxx_i, usxx_i, ucyi, usyi, uczz_i, uszz_i]^T \quad (2-55)$$

where the first subscript represent either the cosine or sine term, the next one or two subscripts represent the deflection in the x, y, or z global directions or the rotations about the global axes, and the final subscript represents the node number. The user can specify several constraints on these deformation components:

- (a) Individual degree of freedom (DOF) can be constrained by specifying the node and direction.
- (b) All DOF can be constrained at selected nodes by specifying the node number.
- (c) A particular DOF can be constrained at all nodes by specifying the DOF number.
- (d) The same DOFs at two nodes can be coupled.
- (e) Rigid links can be placed between two nodes. The user may define "slave" nodes that are tied to "master" nodes. The deformations U_s of the slave nodes are then related to the master node deformations U_m by the transformation:

$$U_s = T_{sm} Y_m \quad (2-56)$$

where, T_{sm} is a transformation matrix defined by:

$$T_{sm} = \begin{bmatrix} 1 & 0 & 0 & 0 & Z_s - Z_m & -Y_s + Y_m \\ 0 & 1 & 0 & -Z_s + Z_m & 0 & X_s - X_m \\ 0 & 0 & 1 & Y_s - Y_m & -X_s + X_m & 0 \\ 0 & 0 & 0 & 1 & 0 & 0 \\ 0 & 0 & 0 & 0 & 1 & 0 \\ 0 & 0 & 0 & 0 & 0 & 1 \end{bmatrix} \quad (2-57)$$

where X, Y, and Z refer to the coordinates of either the master (m) or slave (s) nodes.

There are two restrictions when specifying the slave nodes. First, one node cannot be slave to a slave node, but can share the same master node with other slave nodes. Secondly, an SSI node, the node where SSI loads and coefficients are applied, cannot be a slave node.

The specified constraints are applied to the nodes and DOF numbers are assigned within the code to each of the remaining unrestrained nodes. The DOF numbers are assigned based on the order in which the node numbers are input; therefore, the user should select the node input order for large problems so as to minimize the bandwidth of the stiffness matrix. The bandwidth at each node is printed out during the deterministic analysis to assist in establishing a reasonable input order. For example, if the bandwidth at one node is significantly larger than at other nodes one may consider reordering the nodes so that this node will be located closer to its connecting nodes in the input stream. These DOF numbers are printed out during the deterministic analysis.

Substituting Equations 2-54 and 2-55 into Equation 2-53 yields the following set of linear equations that must be solved at each frequency:

$$\begin{aligned} -M\omega^2 U_c + C\omega U_s + KU_c &= F_c \\ -M\omega^2 U_s + C\omega U_c + KU_s &= F_s \end{aligned} \quad (2-58)$$

There are twice the number of DOF equations in this set. Since the equations are symmetric, only the upper half is stored and all elements outside the maximum bandwidth are eliminated. Solutions are obtained for each frequency using a Gaussian elimination procedure (Bathe and Wilson, 1976).

Once the solutions are obtained the Fourier components of the deformations at user specified nodes are written to a database that can be used in postprocessing to generate response spectra and time history records. Member forces are not evaluated in P-CARES. The volume of output required to assemble member forces is too large to be conveniently treated within a code where simple and fast operation is the primary goal.

2.4.2 Mass Matrix

The mass matrix **M** in the structural analysis module is diagonal and can contain 6 components at each node. A single weight lumped at each node is required as part of the nodal input data, and is used for all 3 mass components M_x , M_y , and M_z . The input weight is divided by the gravitational constant (32.2 ft/sec²) to obtain mass, and hence the length unit needs to be restricted to feet. The weight can be in any units (e.g., kips or pounds) with the restriction that the material property constants such as Young's moduli be in the same force units.

The user can specify rotational masses wherever desired and the rotational masses can be different about the three axes. The rotational masses have the units of [force ft²/sec].

2.4.3 Damping Matrix

The damping matrix **C** in the SSI problem includes the structural component and the SSI component. The structural component used in the structural analysis module is related to the stiffness and/or mass matrices, while the SSI damping component is added directly to the damping matrix **C**. The SSI damping is discussed in the following section when the SSI stiffness is introduced.

There are four options in P-CARES for specifying structural damping. The first three options are based on the fact that the modal equations are uncoupled when the damping matrix is a linear combination of the mass and stiffness matrices:

$$\mathbf{C} = \alpha\mathbf{M} + \beta\mathbf{K} \quad (2-59)$$

where α and β are parameters to be determined using one of the following three options. For the first option the user specifies the value of α and β directly as input. For the second option the value of these parameters are computed within P-CARES based on the first two structural modal frequencies ω_1 and ω_2 (with the base fixed) and a user-specified ratio of critical damping p appropriate for the structure:

$$\begin{aligned} \alpha &= 2p\omega_1\omega_2 / (\omega_1 + \omega_2) \\ \beta &= 2p / (\omega_1 + \omega_2) \end{aligned} \quad (2-60)$$

The first two structural modes are determined by the Power method (Bathe and Wilson, 1976). Both the frequency and mode shapes of these modes are included in the output if a deterministic analysis is performed in P-CARES. The effective structural damping is then equal to the specified damping p at the first two fundamental frequencies but varies from this value at other frequencies. It can be shown that the effective structural damping p_i at some other frequency ω_i is:

$$p_i = p(\omega_i^2 + \omega_1\omega_2) / \omega_i(\omega_1 + \omega_2) \quad (2-61)$$

The damping is less than p for ω_i between ω_1 and ω_2 and larger than p for ω_i outside this range.

In light of option 2, the user may choose two interested frequencies and their associated damping ratio p , use Equation 2-60 to compute values of α and β , and specify these values as input in the first damping option. This approach allows the user to customize the damping characteristics

based on the particular problem under investigation. Equation 2-61 can be used to evaluate the damping value at other frequencies.

Although damping for structural elements is specified during input, it is not used when either of the first two damping types is specified. It is used to determine the **C** matrix when either the third or fourth damping types is specified.

The third type of damping included in P-CARES is termed composite damping (Bathe and Wilson, 1976). It is useful when damping in the various structural elements is different (such as would occur in a structure with both concrete and steel elements). The damping matrix is still defined as a linear combination of the mass and stiffness matrices, but the damping in each of the first two modes is defined as a weighted average of the damping in each of the structural elements, with the weighting function based on the ratio of the strain energy stored in the element to the total energy stored in all of the elements. Therefore, if ϕ_{ij} is the i^{th} modal displacement vector associated with element j , ζ_j is the ratio of critical damping desired for element j , and k_j is the j^{th} element stiffness matrix, the composite damping ratio p_i for mode i is defined as:

$$p_i = \frac{\sum_j \zeta_j \phi_{ij}' k_j \phi_{ij}}{\sum_j \phi_{ij}' k_j \phi_{ij}} \quad (2-62)$$

The parameters used to define the damping matrix in Equation 2-59 are then:

$$\begin{aligned} \alpha &= 2(p_1 \omega_1 \omega_2^2 - p_2 \omega_1^2 \omega_2) / (\omega_2^2 - \omega_1^2) \\ \beta &= (p_2 \omega_2 - p_1 \omega_1) / (\omega_2^2 - \omega_1^2) \end{aligned} \quad (2-63)$$

The fourth damping type in P-CARES relates the damping matrix **C** only to the stiffness matrix **K** by the following equation:

$$\mathbf{C} = -2p\omega\mathbf{K}, \quad (2-64)$$

where p is the damping ratio for an element. This equation is applied in P-CARES in the following procedure:

1. The local stiffness matrix of each element is multiplied by 2 and the damping ratio p for this element, then transformed to the global coordinate system and added to the global damping matrix.
2. As discussed above the final solution is obtained by solving a set of linear algebraic equations at each frequency. Because the damping matrix is frequency dependent, the coefficients of these equations are generated at each frequency by combining the mass, damping, and stiffness matrices. The damping matrix found in the first step is multiplied by the frequency in question and then used to form the coefficients of the dynamic equations.

It should be noted that no extra input is required of the user when this damping type is selected. As stated above the element damping ratio is specified with the element description data. The steps above are executed without user's intervention.

2.4.4 Stiffness Matrix

The stiffness matrix is comprised of structural elements and SSI elements. The structural component to the stiffness matrix is frequency independent; therefore it is formed once and saved to be used during the solution process for each of the frequencies. The SSI component to the

stiffness matrix is generally frequency dependent; therefore it must be computed and added to the stiffness matrix at each frequency in the solution process.

Three structural elements are included in P-CARES: 3-D shear beams, 3-D springs, and shear walls. These structural elements and the SSI contributions to the stiffness and damping matrices are discussed below.

Three Dimensional Shear Beams

Local coordinates for the three dimensional beam model are shown in Figure 2-9. The origin is at the beam start node I and the beam end node is at node J. The local x-axis oriented from start node I to the end node J of the beam. The local z-axis lies in the I, J, and K nodes plane, and the local y-axis is normal to this plane. The section properties must be consistent with the local coordinates. For example, the moment of inertia I_y specified in the input controls bending about the local y-axis or deflection in the local z-axis direction.

The stiffness of the element in the y or z directions is made up of a flexural term and a shear term. The flexural stiffness is related to EI/L^3 and the shear stiffness is related to GA_{shear}/L . The axial and torsional stiffnesses are related to EA/L and GJ/L respectively.

Three Dimensional Springs

Local coordinates for the three dimensional springs are established in the same manner as for the three-dimensional beams as shown in Figure 2-9. Stiffness consists of translational stiffness terms (K_x, K_y, K_z), rotational stiffness terms (M_x, M_y, M_z), and coupling stiffness terms (CP1 through CP6). These data are used to form the following stiffness matrix in local coordinates:

Kx																			
	Ky																		
		Kz																	
			CP1	CP2	CP3														
			CP2	CP4	CP5														
			CP3	CP5	CP6														
			Mx																
				My															
					Mz														
						Kx													
							Ky												
								Kz											
									CP1	CP2	CP3								
									CP2	CP4	CP5								
									CP3	CP5	CP6								
									Mx										
										My									
											Mz								

Shear Walls

The shear wall element is a plane stress quadrilateral element. Each of the four nodes of the element has two active degrees of freedom for in-plane deformations. Since the element stiffness matrices in P-CARES are stored in the global coordinates however, the global stiffness matrix of the shear wall element includes the three deformations in the global coordinate system at each of the nodes. Because the shear wall element has no stiffness resisting out-of-plane deformations or any rotational deformations, these components must be restrained at any node where only shear wall elements contribute to its stiffness.

The shear wall elements can be specified in the input with the material property, four corner nodes, and the wall thickness.

Soil-Structure Interaction (SSI)

P-CARES includes two SSI models, namely for circular and rectangular foundations. The foundation is assumed to be rigid for both types of foundations. Independent of foundation type, soil is assumed as a two-layered system: a layer to the side of the foundation and a layer beneath the foundation. The SSI model makes use of 6 x 6 stiffness and damping matrices to connect the SSI node on the foundation to the free-field. These matrices are generally frequency dependent and are added to the overall structural stiffness and damping matrices. The input motion, i.e., the free-field motion modified by the soil-structure interaction algorithm, is specified as translational and rotational components about each of the global axes. The structure analysis module has more SSI models than the kinematic interaction module; however, if the forcing functions are the generated input motions from the kinematic interaction module, P-CARES will internally choose the same SSI model in the structure analysis module as in the kinematic interaction module for consistency.

Circular Foundation SSI Models

Included in P-CARES are three models for SSI impedance functions for embedded foundations: ASCE 4-98 (1998), Beredugo and Novak (1972), and Pais and Kausel (1985). The first model is frequency independent while the latter two models are frequency dependent. The first model is applicable only for surface foundations; while the latter two models can be applied to embedded foundations. The embedded foundations in these models are restricted to those where the soil can be modeled with two layers, one to the side of the foundation and the other beneath the foundation. This restriction is necessary since analytical SSI impedance functions are not available for more general soil systems. The user can develop "average" soil properties for the two layers in these SSI models from more complex layered soil systems. The original Pais and Kausel data is restricted to the uniform soil case, however is modified in the following manner to treat the case where the soil beneath the foundation has different properties from the soil to the side of the foundation. The SSI coefficients are first determined assuming a uniform soil with the properties of the soil to the side of the foundation. Then, SSI coefficients for a surface foundation (zero embedment depth) are determined for two cases: one assuming a uniform soil with the properties of the soil beneath the foundation and one assuming a uniform soil with the properties of the soil to the side of the foundation. To account for the different properties of the two soil layers, the difference between the solutions of these two cases is added to the initial solution in which the foundation is assumed embedded in a uniform soil. These manipulations are opaque to the user, who is expected to only specify the two sets of soil properties.

Rectangular Foundations SSI Models

The SSI impedance functions for rectangular foundations are computed using the Pais and Kausel model (1985). Pais and Kausel reviewed the available analytic solutions for rectangular foundations and generalized the results so that solutions for the full range of foundation sizes was made available. Static finite element solutions were used to fill in the gaps where data is unavailable, and to generalize the results. The data in Pais and Kausel (1985) is also restricted to the uniform soil case as are most of the available analytic solutions. These data are modified as discussed above to approximate the two layer soil system.

2.4.5 Forcing Functions

By writing the structural displacements relative to the input free-field displacement and by multiplying Equation 2-53 by \mathbf{M}^{-1} , the right hand side of Equation 2-53 becomes:

$$\mathbf{M}^{-1}\mathbf{B}\mathbf{Z}'' = \mathbf{M}^{-1}\mathbf{B}\sum_j (\mathbf{Z}_{c_j}'' \cos \omega_j t + \mathbf{Z}_{s_j}'' \sin \omega_j t) \quad (2-65)$$

where Z = the six components of the free-field displacement (3 translational and 3 rotational)
 B = matrix defining which degrees of freedom are in direction of free-field motion component

In addition to the modified free-field seismic forcing function that is generated from the kinematic interaction module, the structural module allows the user to specify harmonic forcing function at any node in any direction for general purpose structural analysis.

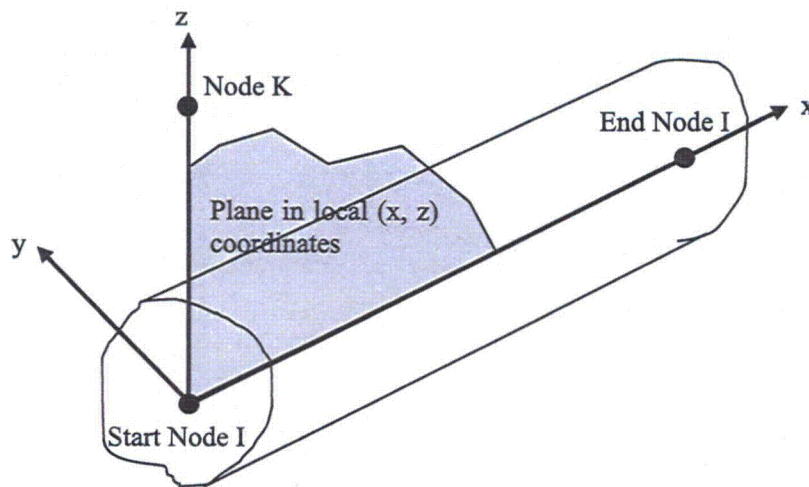


Figure 2-9 Definition of Local Coordinate System for 3-D Beam

2.5 Probabilistic Simulation

Previous sections have discussed the deterministic algorithms to analyze the free-field responses, soil-structure interaction, and the structural responses. These algorithms provides the essential build blocks for the probabilistic site response and SSI analyses since each sample in the probabilistic simulation can be viewed as a new soil-structural system and hence can be analyzed in a purely deterministic sense. This section of the report presents the discussion of adding probabilistic simulation on top of the deterministic algorithms to achieve the probabilistic analyses.

Uncertainties inherent in the soil properties and structural properties can potentially post large variation in soil and structural responses and therefore may have great influence on the inferences obtained during the decision making process. Adequate examination of these uncertainties in the soil and structural system and their impacts on the responses requires a careful layout of the simulation scheme so that the uncertainties can be accounted for with small variation in the statistical estimates and low computational cost. P-CARES includes four sampling schemes for the user to exploit and can be extended straightforwardly if other scheme is in need.

The basic layout of the simulation scheme is illustrated in Figure 2-10, in which P-CARES core on the right side represents the collection of the deterministic analysis modules and all other components on the left side are for probabilistic simulation. All components in the shaded box contribute to yielding a sample (a realization of the random vector). The simulation controller performs a user-specified number of simulation iterations, each of which involves fetching a sample from the shaded box, invoking the P-CARES core to conduct the free-field and/or SSI analysis, and storing the results in database files. The database files are used in post processing and in transferring free-field responses to the structural analysis module.

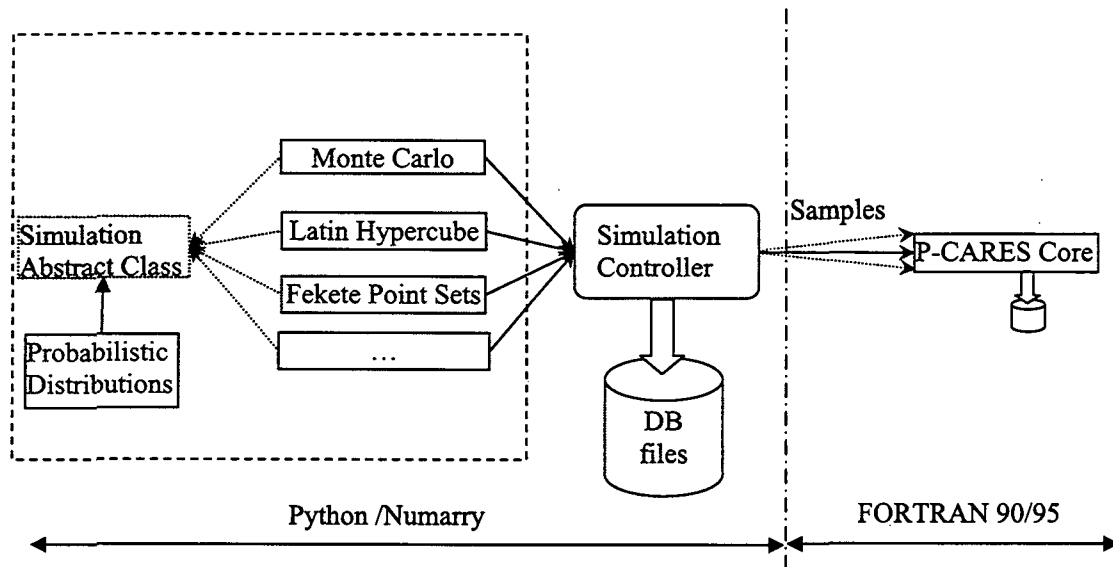


Figure 2-10 Simulation Concepts in P-CARES

The architecture of P-CARES relies on a fundamental procedure that is shared by all simulation schemes in order to streamline the simulation process and to facilitate future addition of other simulation schemes. This procedure will be introduced after a brief discussion of the uncertainty

description, and followed by the introduction of the individual simulation schemes. Post processing will also be briefly discussed at the end of this section.

2.5.1 Uncertainty Description

Because soil properties usually exhibit greater variability than structural properties do, P-CARES, at the stage of current development, considers only the uncertainties inherent in the soil deposit. Random variables are defined as soil density, the low-strain soil shear modulus, and the layer thickness for each layer. Since the material dampings for all soil layers are obtained on the soil degradation curves and to be strain-compatible with the user-specified seismic motion input, it is difficult to include these dampings directly as random variables. However, since each sample soil column has different density and shear modulus properties, the calculated dampings are also different for each sample columns. The layer thickness must be modeled with small variation so that the variation of the total soil overburden can be maintained in a reasonable range.

Lognormal distribution has been chosen to describe the marginal probability distribution for all random variables. It is reasonable when considering that (1) the soil properties are all positive, (2) the difference between a lognormal distribution and a normal distribution is small for small variations (Ang and Tang, 1975, Melchers, 2002), (3) It is sufficient to model the layer thickness by selecting a small coefficient of variation (COV). Assuming all random variables of lognormal distribution also provides a great convenience for describing the layer-to-layer correlations.

Suppose there are N layers in a soil column model, then the total number of random variables is $n = 3 * N$. The number of samples used in the simulation is designated as m hereafter.

An arbitrary correlation between different layers can be specified by the user. P-CARES can rapidly initiates the correlations between soil densities and between soil shear moduli by a simple exponential rule that is similar to the one in Fenton and VanMarcke (1998). For two locations z_1 and z_2 in the soil column, the correlation coefficient is determined by,

$$\rho(z_1, z_2) = \rho_c \min(\exp(1 - |z_1 - z_2| / L_c), 1) \quad (2-66)$$

in which L_c is a user-specified characteristic length to control the influence range, and ρ_c is a characteristic correlation coefficient corresponding to $|z_1 - z_2| = L_c$. The correlation coefficient defined by Equation 2-66 has an upper bound ρ_c . P-CARES calculates an initial characteristic length by averaging the layer thicknesses, and the user can adjust it based on this initial value. The vertical location z_i is selected as the middle point of each layer in P-CARES.

2.5.2 Fundamental Simulation Procedure

The basic probabilistic modeling strategy is to unify different simulation schemes such that the majority of the task can be done in the fundamental procedure. This procedure assumes that an independent uniformly-distributed random vector or independent standard normal random vector is generated first by various simulation schemes. If an independent uniformly distributed vector is supplied, it is first transformed to an independent normal vector by the inversion method. The independent normal vector is then transformed to a correlated normal random vector, which is converted to a lognormal-distributed random vector by taking the exponential of the normal random vector. Individual simulation schemes differ only in how the samples are generated before the correlation is incorporated. The fundamental simulation procedure can therefore be outlined in a method-neutral manner as follows.

Support \mathbf{X} is the lognormal random vector representing the various random properties with mean vector $\boldsymbol{\mu}_X$ and covariance matrix $\boldsymbol{\Sigma}_X$, and \mathbf{Y} is a normal random vector with mean vector $\boldsymbol{\mu}_Y$ and covariance matrix $\boldsymbol{\Sigma}_Y$. The covariance between random variables X_i and X_j , i.e., the (i, j) th entry

σ_{X_i, X_j} in the covariance matrix Σ_X , can be determined using their correlation coefficient ρ_{ij} by the following equation:

$$\sigma_{X_i, X_j} = \rho_{ij} \sigma_{X_i} \sigma_{X_j}, \quad (2-67)$$

where σ_{X_i} and σ_{X_j} are the standard deviations of X_i and X_j . The lognormal random vector \mathbf{X} and the normal random vector \mathbf{Y} are related by:

$$\mathbf{X} = (e^{Y_1}, e^{Y_2}, \dots, e^{Y_n}), \quad (2-68)$$

where Y_i is the i^{th} components in \mathbf{Y} . Equation 2-68 also establishes the relation between the distribution parameters, which can be expressed analytically as in Law and Kelton (2000). The parameter matrices for the normal vector \mathbf{Y} , μ_Y and Σ_Y , can be calculated in terms of those for the lognormal vector \mathbf{X} , μ_X and Σ_X :

$$\begin{aligned} \mu_{Y_i} &= \ln \left(\frac{\mu_{X_i}^2}{\sqrt{\mu_{X_i}^2 + \sigma_{X_i}^2}} \right) \\ \sigma_{Y_i}^2 &= \ln \left(1 + \frac{\sigma_{X_i}^2}{\mu_{X_i}^2} \right) \\ \sigma_{Y_i Y_j} &= \ln \left(1 + \frac{\sigma_{X_i X_j}}{|\mu_{X_i} \mu_{X_j}|} \right) \end{aligned} \quad (2-69)$$

Where μ means a component from a corresponding mean vector μ , σ means a component from a corresponding covariance matrix Σ , a subscript of X_i indicates a component from the lognormal property matrix, and a subscript of Y_i indicates a component from the normal property matrix. Given a correlated normal random vector, one can generate the corresponding lognormal vector using Equation 2-68.

With the mean and covariance matrices μ_Y and Σ_Y calculated from Equation 2-69, the correlated normal vector can be converted from an independent standard normal random vector, denoted as \mathbf{Z} herein, i.e. $\mathbf{Z} \sim N(0, \mathbf{1})$. Since Σ_Y is a symmetric positive-definite matrix, its Cholesky decomposition \mathbf{C} exists such that $\mathbf{C}^T \mathbf{C} = \Sigma_Y$. Then, the dependent normal random vector is generated by the following equation,

$$\mathbf{Y} = \mathbf{C}^T \mathbf{Z} + \mu_Y. \quad (2-70)$$

The independent standard normal random vector can be generated by using a normal generator or by using a uniform generator and the inversion transformation method. The later approach is more flexible because it allows methods such as Fekete Point Sets method to be used.

The inverse of the above derivation procedure institutes the fundamental simulation procedure. All simulation schemes introduced in the next section share this procedure beyond their different ways to generate the independent normal or uniform random vectors.

2.5.3 Simulation Schemes

Four different simulation methods have been implemented P-CARES, including Monte Carlo method, Latin Hypercube sampling method (LHC), Engineering LHC, and Fekete point sets method. Except for the Monte Carlo simulation that directly generates independent normal

vectors, all other schemes generate independent uniform vectors and then use an inversion method to generate the independent normal vector.

Given a realization u of a uniform random variable $U \sim U(0,1)$, a normal sample z of a corresponding normal random variable $Z \sim Z(0,1)$ can be generated by,

$$z = \Phi^{-1}(u), \quad (2-71)$$

where Φ^{-1} is the inverse of the normal cumulative distribution function (CDF). Inversion of Φ cannot be accomplished analytically, and its numerical solution involves iteration and numerical integration and therefore is very demanding in computation. P-CARES uses a recent method using rational approximation by Acklam (2000) to obtain this inverse. The relative error of this method is reported less than 1.15×10^{-9} for z in the range $[-38, 8.20954]$; beyond this range, the uniform sample u is either too small to be represented accurately or simply unity using the current IEEE double precision real number. Therefore, this method bears no practical limitation, and the level of accuracy is adequate in the particular application of this report because the simulation occurs in the central region of the random variable space. The particular version used is a Python implementation published on the author's website.

Monte Carlo Simulation

The Monte Carlo simulation implemented in P-CARES uses the native standard normal generator contained in the Python Numarray module, which is an algorithm in Ranlib developed by Ahrens and Dieter (1973). Ranlib is a selection of C routines to generate random numbers from various distributions. Since this algorithm generates independent normal numbers, the task left in the Monte Carlo simulation is simply to generate n samples that serve as Z in Equation 2-70.

Latin Hypercube Sampling

Monte Carlo simulation requires a large number of samples to get a reasonably converged estimate, i.e., with a reasonable low variation. Among various variation reduction techniques, Latin Hypercube sampling technique has been widely used in many different domains that involve simulation (e.g., McKey et al, 1979, Nie, 2003, Wyss and Jorgensen, 1998). Following the fundamental simulation procedure, the purpose of Latin Hypercube sampling in P-CARES is to generate m sample vectors in n dimensional hypercube. It starts with dividing the range $[0,1]$ of each uniform random variable U_i into m nonoverlapping intervals (with equal probability). One value u_{ij} is then randomly selected from each interval, where j indicates the value from the j^{th} interval. The m values of all random variables are combined randomly to form m LHC samples, each contains n values as a realization of the random vector of size n . It should be noted that any of the m values of any random variables is used only once in forming the m LHC samples. The quality of one particular set of m LHC samples depends on how evenly these samples are distributed in the n -D hypercube.

The above generation procedure is clarified by the following example. Suppose that the size of the random vector $n = 2$, and the number of samples desired is $m = 5$. Figure 2-11 shows two equally possible sets of the LHC samples. The small solid dots are the randomly selected values in the 5 intervals for each random variable, while the hallow stars are the 5 LHC samples, each of which is a combination of one value from each random variable. The LHC samples shown on the left side are better than the ones on the right side because they are scattered more evenly.

The generated LHC samples in the hypercube are transformed to samples in standard normal space by Equation 2-71. Finally, the fundamental simulation procedure is applied to get the lognormal sample vectors.

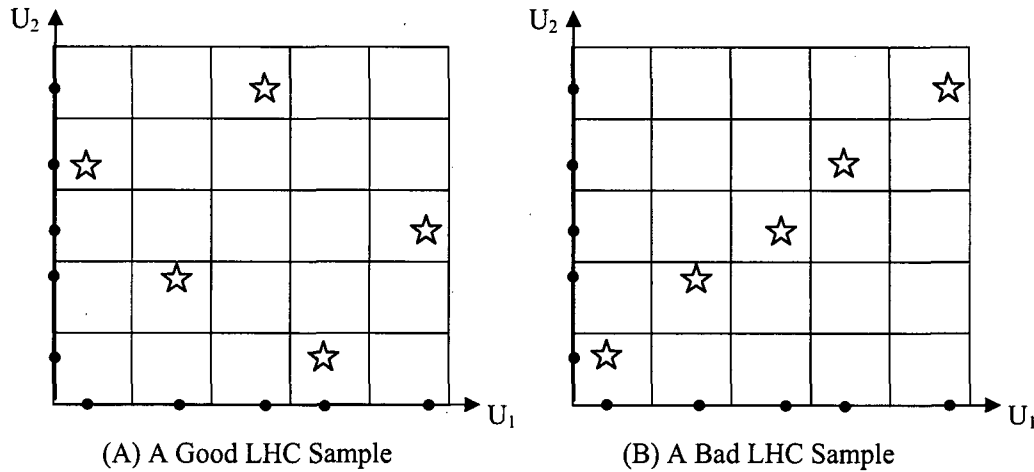


Figure 2-11 A 2-D Latin Hypercube Sample

Engineering Latin Hypercube Sampling

Rather than selecting randomly a value in each interval, as described above in the conventional Latin Hypercube sampling technique, a common practice in engineering application of LHC is to select the median point in each interval. This revised version, termed as engineering LHC here, removes the randomness in the marginal samples if each individual random variable is under consideration. However, the LHC samples, as random combinations of the marginal values of all random variables, still exhibit great randomness. The engineering LHC can avoid some extreme values close to the boundaries of the hypercube.

Fekete Point Set Method

Fekete Point Set method was developed as an advanced directional simulation tool in assessing structural system reliability (Nie, 2003). Fekete Point set is a set of points on the unit hypersphere with a minimal potential energy, i.e., it minimizes the following potential energy,

$$E_t = \sum_{1 \leq i < j \leq m} \frac{1}{|\mathbf{P}_i - \mathbf{P}_j|^t}, \quad t > 0 \quad (2-72)$$

Where t is the order of the potential energy E_t , \mathbf{P} represents a point on the unit hypersphere, and m is the total number of point in the set. Among the three generation methods developed in Nie and Ellingwood (2004), the one directly minimizing E_2 has been adopted in P-CARES. Detailed discussion of these generation methods is beyond the scope of this research. In the particular applications in evaluating structural system reliability, the method was assessed in spaces of a dimension up to 20. The authors noticed that the advantage of Fekete Point set method over Monte Carlo simulation decreases as the dimension increases, from about several hundreds times more efficient in 3-D to about 3 times more efficient. Spaces of a dimension higher than 20 have not been tested. Therefore, this method is included in P-CARES as an experimental approach, and the user should use it with caution.

A Fekete Point set is on the unit hypersphere, and must be transformed into the hypercube to be useful in P-CARES. Such a transformation developed in Nie (2003) has been incorporated together with the generation procedure in P-CARES. When generating a Fekete Point Set in P-CARES, this transformation is automatically applied at the end of generation without user's intervention. A fact of this transformation is that an $n+1$ dimensional unit hypersphere maps to an n dimensional hypercube, because hypersphere has one degree of freedom constrained by its

radius. A visual comparison between Fekete point set and LHC samples is presented in Figure 2-12, in which Fekete point set does not have the tendency of point clustering as observed in some of the LHC samples, and therefore can be viewed as scattered more evenly. The reordered Fekete points are similar to the Fekete points except that they have their marginal values same as in the engineering LHC.

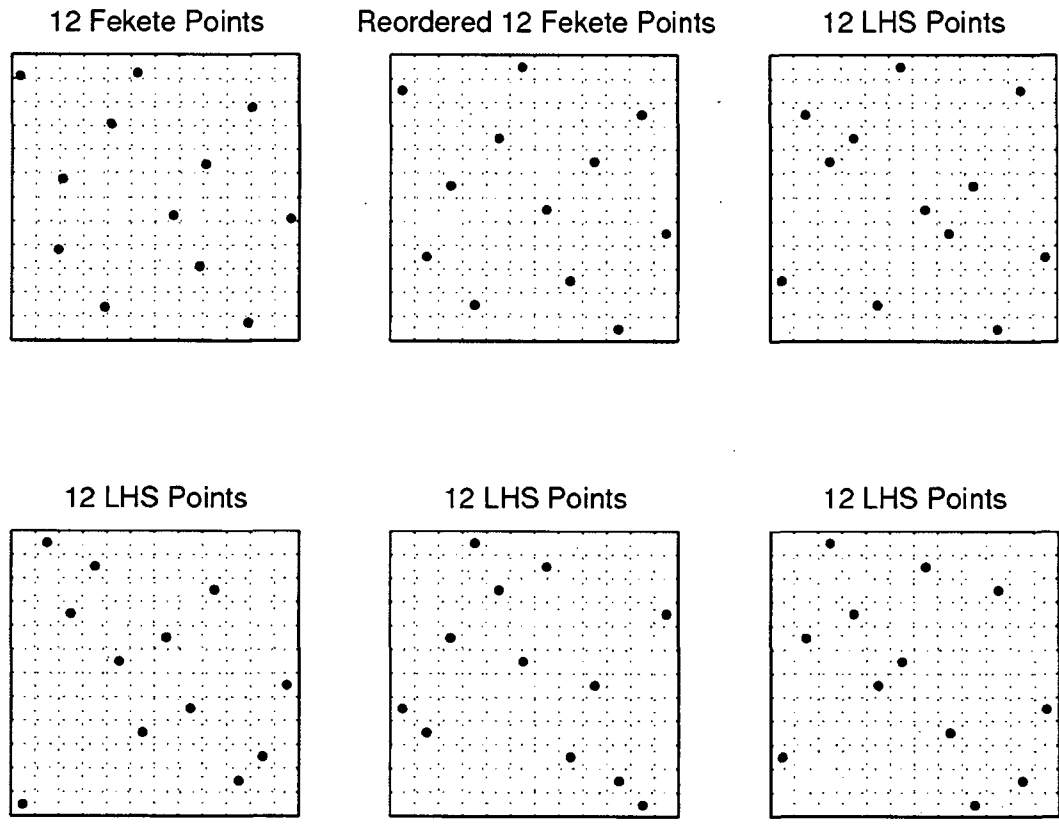


Figure 2-12 Comparison of 12 Fekete Points and LHC Points (Nie, 2003)

2.5.4 Post Processing

Post processing module in P-CARES provides various statistics on the simulation results. For soil profiles, the mean, median, minimum, maximum, and arbitrary percentiles can be generated from the sample profiles. For the responses, response spectra can be generated using a user-specified damping value and be presented as the mean, median, and user-specified percentiles. The response spectrum of the input motion can also be included in the output (see Figure 2-13).

Except for the sample mean that is taken as the arithmetic average of the samples, other statistics are all based on a percentile algorithm. The samples are first sorted and then the p -percentile value is simply defined by the following index function,

$$I(p) = \text{round}(p * m / 100), \tag{2-73}$$

where m is the number of samples in the simulation, and $\text{round}()$ is a function that rounds a real value to the nearest integer, $I(p)$ is the index that points to the data in the sorted samples. The indices of other statistics are defined as,

$$\begin{aligned}
 I_{\min} &= I(0) \\
 I_{\max} &= I(100) \\
 I_{\text{median}} &= I(50)
 \end{aligned}
 \tag{2-74}$$

For deterministic analysis, the outputs are the free-field responses and the SSI responses at various locations of the structure. These outputs, in Fourier components format, are saved as individual text files. Therefore, the post processing task for deterministic analysis can be achieved by utilizing the seismic motion utility module.

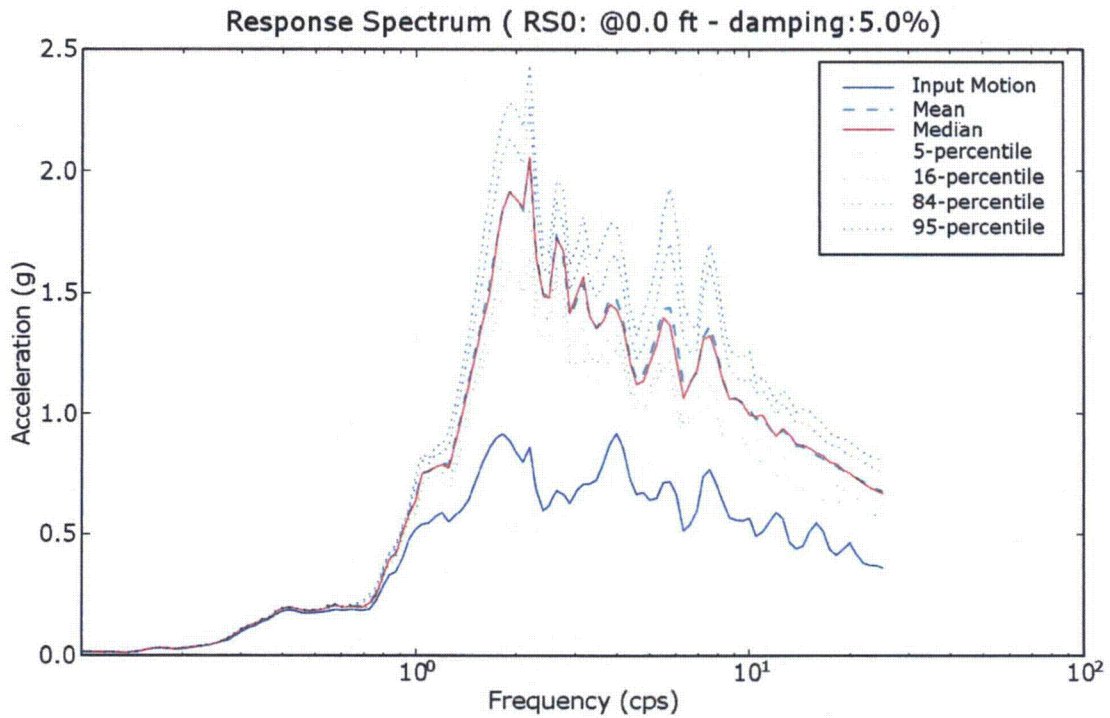


Figure 2-13 Statistics of Response Spectra in Post Processing

3 SEISMIC ANALYSIS FEATURES OF P-CARES

The P-CARES program consists of many components that either are adopted from the earlier versions of CARES codes or are recently developed. The codes adopted from CARES are re-modulated so that these modules can be called individually at appropriate situations in the deterministic and probabilistic analyses, and become the computing core for the free-field analysis and soil-structure interaction (SSI) analysis. Building on these upgraded codes, a significant amount of effort has been made to manage the calculations necessary for deterministic and probabilistic analyses, to generate random vectors that are used in the probabilistic simulation, to construct the graphical user interface (GUI) that facilitates data input, calculations, and post processing, and to provide interfaces that connect the modules in the computing core to the GUI and the probabilistic management modules. With this integrated package of components, P-CARES can provide both deterministic and probabilistic free-field response and SSI analyses in a very efficient way. This section summarizes the functionalities which are implemented in P-CARES.

Although consideration for multiple platforms has been given during the development of the P-CARES program, it has been so far compiled and tested only on Windows XP, currently the most common operating system. P-CARES has been developed using a mixed programming approach that involves FORTRAN 90/95 and Python programming languages. FORTRAN 90/95 is used for the computing core that involves heavy number crunching; while Python is used for the probabilistic modeling, data and file management, and GUI development, as these functions do not consume much computing time. The FORTRAN 90/95 modules and subroutines are compiled to Python modules using the open source tool f2py that collaborates with the Compaq Visual FORTRAN 6.6 and the Microsoft Visual C++ .Net 2003 in the P-CARES development. In particular, the GUI was developed with wxPython, a Python binding to the open source C++ wxWidgets graphical toolkits. Another open source package, named matplotlib, was utilized with an extended toolbar to produce and manipulate various plots. The python port of the 3-D graphical toolkit VTK 5.0 was used for the 3-D structural model viewer. A GUI layout tool, wxDesigner, is used in the P-CARES development to expedite the GUI design and programming.

On Windows XP, P-CARES can be started by simply double-clicking the icon in the "All Programs" folder. During the time the splash screen is exhibited temporarily on the window screen (see Figure 3-1), P-CARES loads all the functional modules and then displays the main GUI for user's input and control. Various functions can then be performed within the GUI. The GUI will be overviewed first to establish the context in which other functionalities can be described later. The utilities to manipulate accelerogram, the deterministic analyses, and the probabilistic analyses are then explained in sequel.

3.1 Graphical User Interface

All functionalities of P-CARES can be executed through its main window, as shown in Figure 3-2. This subsection provides only an overview of the basic layout and major functions that can be referred to when other soil and structural analyses capabilities are introduced. More detailed description will be presented in Section 4 of this report.

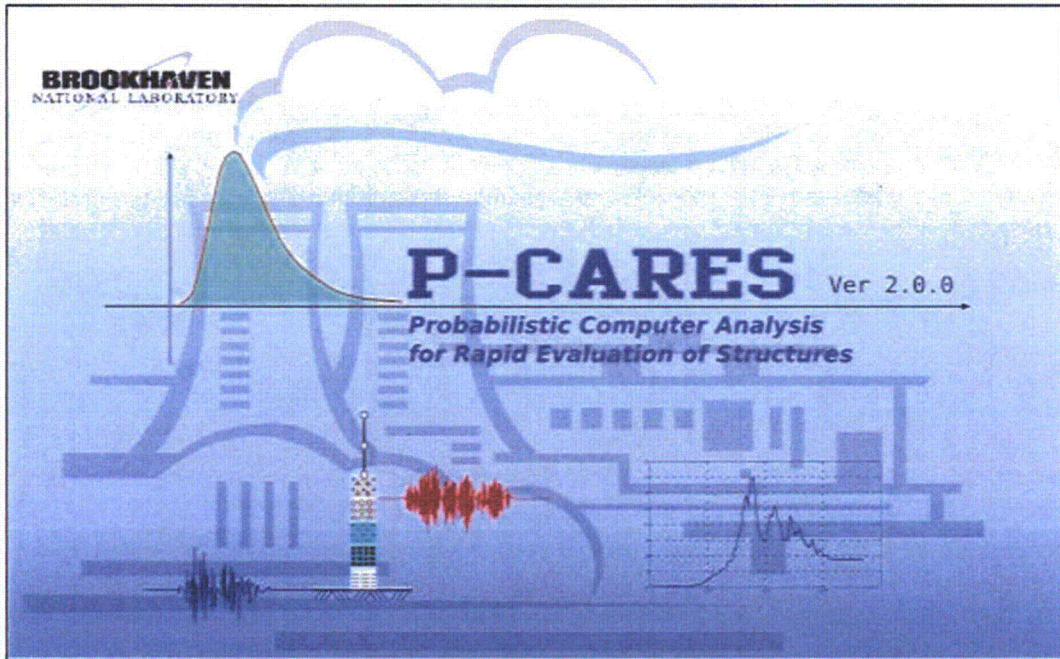


Figure 3-1 P-CARES Splash Screen

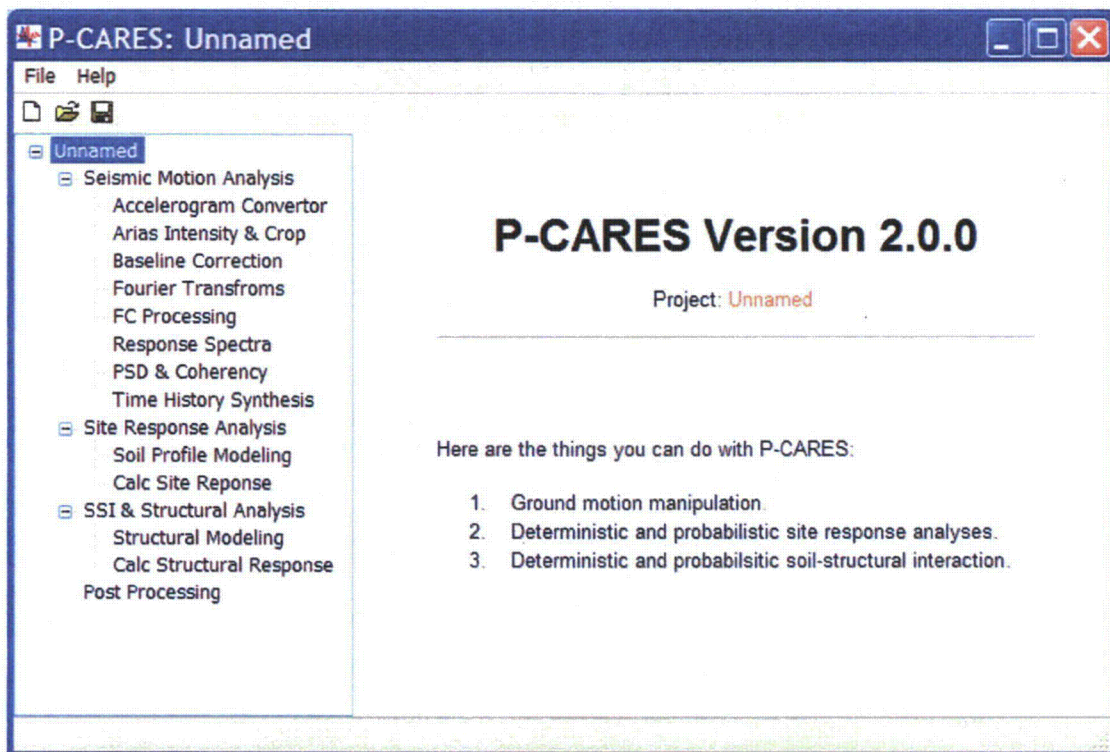


Figure 3-2 P-CARES Main GUI

The main GUI consists of a menu bar, a toolbar, a hierarchical panel of various functionalities on the left, and the main display panel on the right. Toolbar buttons and menus are used to create, open, and save a project. A project means a collection of files in the project's directory, which

contains a main input file and other associated files such as input seismic accelerograms, output files, and database files. If a project has been created or opened, its name is displayed at the root of the function panel; otherwise, it is named as "Unnamed".

The hierarchical panel, developed based on a tree structure, contains all the links to various sets of functions provided by P-CARES. These functions are organized into four major groups, namely the seismic motion analysis, the site response analysis, the SSI and structural analysis, and the post process. When a link is activated by pointing the mouse on and clicking the link, the corresponding interface will be displayed in the main display panel, which may be a pure data input panel or a console panel that takes user input and generate outputs (plots). The general layout of a console panel includes a plot panel on the top and some controlling features at the bottom (For example, Figure 3-3). The analysis methods, deterministic or probabilistic, can be specified as options in the site response and SSI analyses modules, as shown in the Figure 3-2. The manner in which the analyses are categorized as the site response analysis and the SSI and structural analysis reflects the common practice that these two types of analyses are often performed separately regardless of deterministic or probabilistic analysis. However, this arrangement does not rule out the successive execution of these analyses in either a deterministic or a probabilistic calculation.

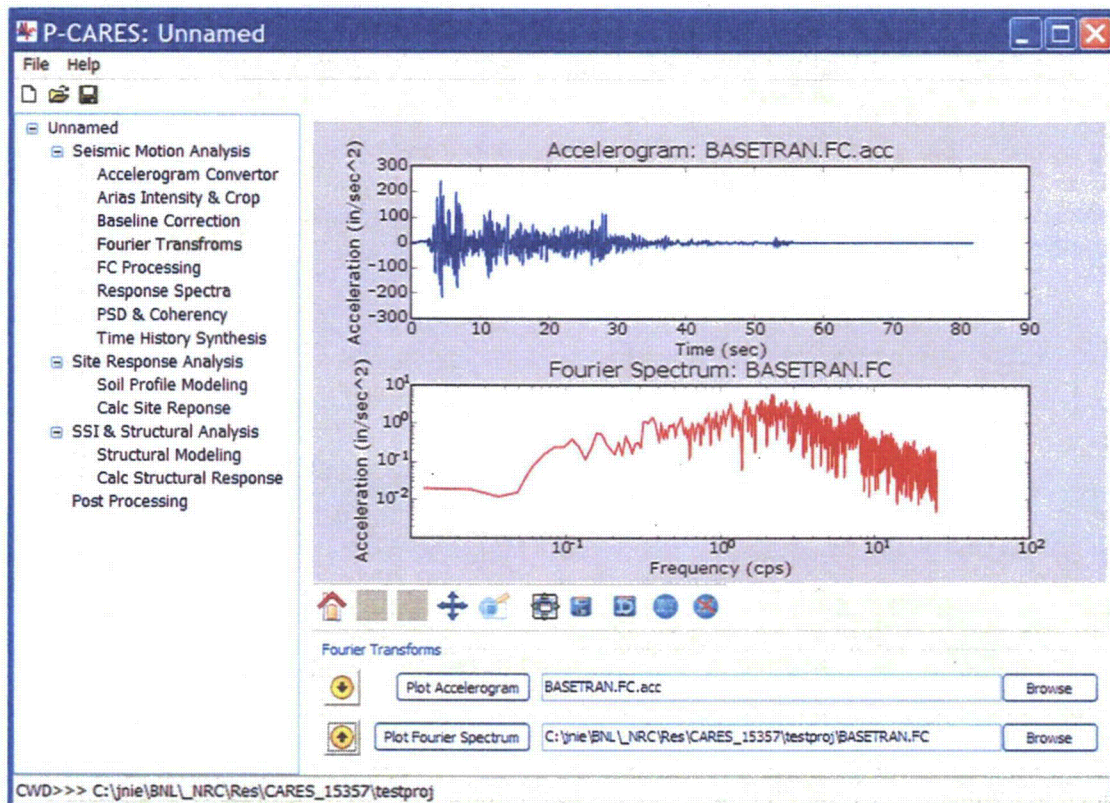


Figure 3-3 A Typical Console Panel Shown in the Main Display Panel

The basic approach to using P-CARES is: (1) to process seismic motions using the provided utilities, (2) to prepare input for the soil column using the soil profile modeling and to conduct the site response analysis by selecting an option for either deterministic or probabilistic analysis, (3) to build the structural model using the structural modeling tool and to perform the SSI and

structural analyses. The last step can acquire the calculation type, i.e., either deterministic or probabilistic, from step (2) and perform a joint SSI analysis, or can be executed as an independent analysis by directly specifying input motion and SSI coefficients.

In contrast to the traditional programs such as the previous CARES versions that use special file format to organize various data, P-CARES does not require the user to prepare the input in a particular data file format, except for some auxiliary files such as accelerograms and their Fourier component files, because the input data can be entered and edited through the GUI. Those accelerograms and their Fourier component files hold bulk data that are seldom processed manually, and therefore maintain the existing file format with minor improvements.

A toolbar attached to the bottom of the plot panel facilitates the manipulation of the plot, which allows panning, zooming, setting the margins of the plot, annotating the plot, and saving the figure and the data. All these functions will be described in more detail in the user's manual.

3.2 Seismic Motion Analysis

As the first group in P-CARES and often the first step in a typical analysis session, a set of utilities are provided for the user to preprocess the input seismic motions and to perform some of the post processing tasks, especially for the deterministic analysis. These utilities, grossly organized in an order convenient for typical analysis situations, include a accelerogram convertor that converts a raw acceleration time history in various formats to P-CARES format, a utility that displays the accumulative Arias Intensity and can save a portion of the whole time history by chopping and zero-padding, a baseline correction utility to remove the residual velocity and displacement from a time history, a utility that performs forward/inverse FFT and generates relevant plots, a FC processing utility that can filter or smooth a given Fourier component file, a response spectra utility that can handle multiple damping values, a power spectra density and coherency utility, and a time history synthesis utility to generate a time history that matches a given response spectrum. These utilizes are described in the following.

3.2.1 Accelerogram Convertor

Accelerograms obtained as either recorded data or artificial time histories are in different format in practice, and cannot be universally accepted in P-CARES without conversion. This utility converts a raw record into P-CARES format. The raw records are required to be in text format with all acceleration data organized in one or more columns and evenly spaced in time. This convertor can retrieve acceleration data that are either separated with arbitrary delimiters or assumed in fixed widths.

A raw accelerogram file can be opened and displayed for inspection and an appropriate delimiting method can be determined accordingly. After a raw file is opened and an appropriate delimiting option is selected, the user can parse the file to display data fields colored column-wisely. Certain unwanted rows in the file can be commented out conveniently. A second parse identifies all accelerogram data in the file after every accelerogram data field is clicked in an arbitrarily selected row. The user can specify the time increment and the conversion factor from the unit in the raw accelerogram into in/sec^2 used in P-CARES format, plot the whole record, and pick a range on screen for saving. The processed accelerogram in P-CARES format can be saved to a user-specified file name, which has a default file name by suffixing the input file with ".acc" to avoid accidentally overwrite the original file of the raw record.

3.2.2 Arias Intensity and Crop

As discussed in the theory section, Arias Intensity is a good measure of the seismic energy content, and can be used to identify the strong ground motion in the whole accelerogram. In practice, an intact seismic accelerogram may have very long duration and require an unnecessary extra computing cost if unchanged. Therefore, the accelerogram often needs to be shortened by chopping off its beginning and end portions. This tool can display the accelerogram on the screen, calculate the cumulative Arias Intensity, show typical percentiles of Arias Intensity for reference, and dynamically show the start and the end positions for chopping. The chopped accelerogram is automatically saved under a file name that prefixes the original accelerogram file name with "cropped_", which ensures the original file does not be overwritten accidentally. The user can also specify the length of zero padding at the beginning and the end of the cropped accelerogram.

The accelerogram files are customarily named with an extension ".acc".

3.2.3 Baseline Correction

Seismic accelerograms, either recorded or synthetic, often have nonzero residual velocities and displacements, which are mostly fictitious or unrealistic but need not to be corrected in many cases in which the nonzero residual velocity and displacement do not affect the calculation result. In some other cases, however, these residual velocity and displacement do affect the calculation adversely, and therefore must be removed. This utility can read in an accelerogram and correct it using a Lagrange multiplier based minimization method published by Borsoi and Ricard (1985). This utility can plot the original and corrected accelerograms, the corresponding velocity and displacement histories, and their Fourier spectra. These plots visually inform the user the effects of the correction on the accelerogram and the Fourier content. Only minor changes to the original accelerogram have been observed using this method. The corrected accelerogram is automatically saved in a file name with the original file name prefixed with "bl_".

This utility also saves, as a side effect, the Fourier spectra for both the original and the corrected records, under file names of the accelerogram file names plus ".fc", which means the Fourier Component format.

3.2.4 Fourier Transforms

This utility performs the forward and inverse FFT and displays the time history and its Fourier components. Individual accelerogram or Fourier component file can be displayed as well. The generated pertinent file is saved in a file name with the original file name being suffixed either with ".acc" or ".fc" depending on whether a forward or inverse transforms is performed.

3.2.5 FC Processing

This utility can read in and display a Fourier component file as its first function to inspect the Fourier spectra, and provides a Butterworth filter function and a smoothing function.

The Butterworth filter function can be a low pass, high pass, or a bandwidth pass filter depending on whether the corresponding cutoff frequency is set to zero. A zero cutoff frequency turns off the corresponding filter function, for example, if the low cutoff frequency is zero but the high cutoff frequency is not, then the Butterworth filter becomes only a low pass filter. The filtered Fourier spectrum is plotted overlaying the original in real time. If the filtered version is saved, its file name is obtained by adding a prefix "bw_" to the original file name.

A smoothing function is also provided in this utility using a triangular window, either with a fixed frequency window width or a varying window width. The smoothing window width, in terms of

frequency (Hz) for a fixed window with option or percentage (%) of the center frequency, can be specified by the user. The smoothed version is displaced instantly on top of the original after clicking the “Smooth” button. If saved, its file name used is the original file name prefixed with “sm_”.

The Butterworth filtering and the smoothing function can be applied together, although it is not a common practice. These two functions can also be applied for multiple times to achieve the desired result. The filtered and/or smoothed Fourier components can be transformed into time domain and be saved using the appropriate prefix and suffix.

If the processed Fourier components sequence is transformed to time domain, it is saved in an accelerogram file with its name obtained by simply adding an extension “.acc” to the original Fourier component file. The combination of this utility and the baseline correction utility or Fourier Transforms utility introduced above can produce chained file names as “.acc.fc.acc...”. This special arrangement can potentially create many files if the mentioned utilities are executed multiple times, however it is regarded as a safe measure that prevents the possibility to overwrite a file by accident. Nevertheless, this feature should not be considered awesome because deleting files is such an effortless task on any modern operating system.

3.2.6 Response Spectra

This simple utility reads in an accelerogram and generates the response spectra for a list of user specified dampings. These response spectra curves are plotted on screen using different colors, and are saved to individual files. The file name for a response spectrum using damping d is created as the original accelerogram file name suffixed with “rs d ”. For example, if the damping used is 5% and the original accelerogram file is “record.acc”, the file name for the response spectrum is “record.acc.rs5”.

3.2.7 PSD and Coherency

This utility reads in one or two accelerograms and plots their power spectra density functions as its simplest usage. More importantly, it is a tool to calculate the various coherency measures and to create the corresponding plots. The user can specify the size of the tapering function that is applied to the time history and the width of the Hamming window for locally smoothing the auto and cross power spectra before the various coherency measures are calculated. The included coherency measures are the lagged coherency, the phase spectrum, the unlagged coherency, and the Arctanh coherency.

The various plots can be saved in a variety of common image format or in a two-column format by using the plot toolbar.

3.2.8 Time History Synthesis

This utility generates an accelerogram that matches a given response spectrum. The shape of the synthetic accelerogram is made to be closer to a realistic record using an envelop function, which is defined by the user-specified earthquake magnitude estimate M . The record is also automatically baseline-corrected using the Lagrange multiplier based correction tool and enveloped by the maximum peak ground acceleration specified by the user. The target spectrum can be selected to be one of the NUREG-CR0098 (Newmark and Hall, 1978), RegGuide 1.60, or a user specified spectrum. The response spectra are linearly interpreted in the log-log scale.

After specifying the number of iterations, the duration, the number of data point, optionally the rise/strong/decay times, and importantly target spectrum, and the phase generation method,

clicking the “Initialize” to start the generation process. An artificial time history can be generated by clicking the “Synthesis” button for one or more times, each of which iterates the specified number of iterations based on the previous generated or initialized time history. After each clicking, the response spectrum of the synthetic accelerogram is plotted over the target response spectrum and the synthetic accelerogram is plotted over the envelop function. By visually checking the level of the agreement between the artificial response spectrum and the target spectrum, the user can decide if more iterations are needed or a completely new record is generated by reinitialize the utility. A Regguide check can be performed to ensure the synthetic time history in line with the requirement of Regulatory Guide 1.60.

The phases can be generated randomly or by reading an existing record that is stored in either Fourier component.format or in time history format. If an option of a time history is selected, the time history is first transformed internally to the Fourier components and the phases are then extracted. To maintain compatibility, the duration and the number of points for the synthetic time history are fixed to those of the existing accelerogram if it is used for phase generation.

The acceleration, velocity, displacement, and the response spectra of the synthetic time history can be saved in individual files of file names that can be specified by the user. These file names are initialized as SYNTH.acc, SYNTH.vel, SYNTH.disp, and SYNTH.RS in default.

3.3 Deterministic Free-Field Response and SSI Analysis

Upon the preparation of the seismic motions, the user can continue for deterministic free-field response analysis and SSI analysis. The free-field response analysis and the SSI analysis can be performed independently or jointly; therefore, there are three analysis scenarios for the deterministic analysis: (1) independent deterministic free-field response analysis, (2) independent deterministic structural analysis that includes options for the standalone SSI analysis and the frequency domain shaker analysis, and (3) joint deterministic free-field response and SSI analyses. For the first type of analysis, it is sufficient to select the analysis type as “Deterministic” in the calculation panel of site response analysis. For the second type of analysis, there are an option for the standalone deterministic SSI analysis and an option for the frequency domain shaker analysis in the calculation panel of the SSI and Structural analysis. For the last type of analysis, it is required to select “Deterministic” analysis in the free-field response analysis and to select the “Joint SSI” analysis in the structural analysis panel. The user can build the soil column model and the structure model, perform the various calculations, and post process the outputs all through the GUI.

The following is a list of the main features provided for the deterministic analysis.

- + The soil column is assumed to be a one dimensional layered soil system with the shear wave propagating vertically through the soil layers. The nonlinear behavior of the soil is modeled with specified soil degradation curves and the input seismic motion; the resultant soil shear modulus and damping of each layer are compatible with the maximum effective strain incurred by the input seismic motion.
- + The user can specify the number of layers, soil degradation model, soil layer properties, water table, rock properties for rock outcrop, input seismic motion and its location of application, output locations for free-field responses, and a file name used to store the final strain-compatible soil profile.
- + The input seismic motion can be placed at the ground surface, at any layer interface, or in the rock outcrop.

- + The soil layer properties include the layer thickness, soil weight density, soil shear modulus, and soil type, which can be entered and edited in the main GUI.
- + If a joint SSI analysis is to perform, the user should also provide the foundation type, dimension, and the embedment depths in the soil modeling stage. The inclusion of the kinematic soil-structure interaction in the site response analysis can be turned on or off by a simple option. P-CARES will automatically generate the side and base soil properties from the input soil column profile, record the output motions at locations spanning over the embedment depth, and then generate the SSI input motions.
- + The structure is a lumped mass linear elastic structural system, which consists of beam elements, spring elements, shear wall elements, and the rigid link elements. A P-CARES beam element is a 3 dimensional beam with shear stiffness enabled, while a spring element is a 3 dimensional beam without shear capacity. The shear wall elements cannot resist any out-of-plane deformation and rotational deformation.
- + The structural model can be viewed and inspected in the 3D viewer.
- + The user can specify the nodal definitions and constrains, coupled degrees of freedom, rigid links, element type and connectivity, material properties, sectional properties, the damping model and parameters, and SSI node for all deterministic structural analysis.
- + The user can specify SSI model, foundation type and dimensions, base and side soil properties, if a standalone deterministic SSI analysis or a frequency domain shaker analysis is to be performed.
- + The user can specify the input motions in any or all of the six directions at the SSI node for a standalone deterministic SSI analysis.
- + The user can specify the forcing function at any given node and direction for a series of user specified frequencies, if the frequency domain shaker analysis option is selected.
- + For a joint SSI analysis, P-CARES internally sets the SSI model to Beredugo and Novak model (1972) for circular foundations or Pais and Kausel model (1985) for the rectangular foundations. The input motions are taken automatically the translational and rotational kinematic motions generated in the site response analysis, and the side and base soil properties are derived from the final soil profile saved in the site response analysis.
- + The user can specify a list of nodes at which the output motions need to be recorded. The output motions are in the Fourier component format.
- + The output motions, including the free-field responses at various depths in the soil deposit or in the rock outcrop, and the structural responses at various nodes in the structural model, can be processed using the seismic motion analysis utilities. These output files are in text format.

3.4 Probabilistic Free-Field Response and SSI Analysis

The probabilistic free-field response analysis can be activated in the site response calculation panel, and the probabilistic SSI analysis can be activated by selecting the “Joint SSI” analysis in the structural calculation panel in conjunction with a probabilistic site response analysis. Because the structural components are considered to have less variability than soil properties, they are currently modeled deterministically; therefore, the probabilistic SSI analysis is simply to pass the uncertainties in the soil to the structural responses. There are two types of analysis: (1) independent probabilistic free-field response analysis, (2) joint probabilistic free-field response and SSI analyses.

A large portion of the data input is shared by the probabilistic analysis and the deterministic analysis. The additional data required for the probabilistic analysis include the probabilistic distribution data (mean and standard deviation) for soil weight density, soil thickness, and soil

low strain shear velocity of each layer, and the layer to layer correlation data. Although P-CARES takes the shear velocities as the input random variables, the shear moduli are in deed the internal random variables in the calculation. The lognormal probabilistic distribution is assumed for all random layer properties. The uncertainties of the layer properties can be specified by either the standard deviation (Std) or the coefficient of variation (COV). Arbitrary feasible and compatible correlation can be specified between any layer properties. A simple tool, based on a rule of exponential spatial variation as described in Section 2, can be used to initiate the correlation table for soil weight density and soil shear modulus between adjacent layers.

For probabilistic analysis, P-CARES implements four simulation schemes, i.e., Monte Carlo simulation, Latin Hypercube sampling, engineering Latin Hypercube sampling, and the experimental Fekete Point set method. The user can select the simulation method in the site response calculation panel, and specify the number of samples used in the simulation. Fekete point set can be specified with a previously stored file or can be generated on the fly. The dimension of the random vector is the triple of the number of the soil layers. The number of samples used in the Fekete Point set method is required to be greater than the number of random variables in the simulation.

The generated SSI input motions, one translational and one rotational at the base of the foundation, are stored in a binary database file and are used to supply the input motions to the structural model. The final soil profiles for all samples are stored in their own database file as well, which is used to generate the SSI coefficients for the structural model. The output motions, including those in the soil deposit and at the nodal locations in the structure, are stored as Fourier components in two separated database files, which are used in the post processing to generate response spectra for various percentiles.

The post processing in the probabilistic analysis merits its own module because of the necessary statistics calculation. This module provides post processing capability for soil profile and output motions. For soil profiles, profiles at the mean, minimum, maximum, median, and other arbitrary list of percentiles can be plotted and saved. Each soil profile includes properties of layer thickness, soil density, damping, initial shear modulus, final shear modulus, initial shear velocity, and final shear velocity. For output motions, the response spectra at the mean, median, and various percentiles can be plotted and saved. There is an option to include the response spectrum of the input motion as a solid blue line in the response spectra plots. All statistics plots obey the following codes of color and line style:

- + *Mean*: cyan dashed line (thick, 1 pt)
- + *Minimum*: green solid line (fine, 0.35 pt)
- + *Maximum*: blue solid line (fine, 0.35 pt)
- + *Median*: red solid line (0.5 pt)
- + *50+ Percentile*: blue dotted line (fine, 0.35 pt, varying color)
- + *50- Percentile*: green dotted line (fine, 0.35 pt, varying color)

